1
Introduction

C.A. Foss

ABSTRACT

This book presents studies from geological mapping and mineral exploration projects for which delivery of practical solutions was paramount. Individual chapters are self-contained, with Chapters 2 to 4 largely focusing on estimation of depth to magnetisation and Chapters 5 to 15 investigating issues related to magnetic field expression of remanent magnetisation. The qualitative interpretation of geology from magnetic field imagery is well covered by Isles and Rankin (2013) and we do not address that topic here. Fundamental mathematics supporting magnetic field interpretation is explained in 'Potential theory in gravity and magnetic applications' (Blakely 1995) and additional background information can be found in 'Aeromagnetic Surveys: principles, practice and interpretation' (Reeves 2005) and 'Gravity and magnetic exploration: principles, practices, and applications' (Hinze *et al.* 2013). Rock magnetism and palaeomagnetism are well described in the textbook 'Palaeomagnetism: magnetic domains to geological terranes' (Butler 1992) that is freely available on the internet and Clark *et al.* (2003) review the geological controls on rock magnetism and their significance in mineral exploration. The role of magnetic field methods in mineral exploration projects where they are combined with other geophysical techniques is described in 'Geophysics for the mineral exploration geoscientist' by Dentith and Mudge (2014).

At the time of writing this book there is a pressing need for discovery of new metal deposits to replace those we are exhausting, particularly in support of the transition to a low-carbon economy. Conferences and publications by geophysical societies across the world bring together government, company and academic geoscientists and play a key role in enabling the discovery of new mineral deposits. These discoveries require drilling and drilling requires models. The current expectation of many geophysicists in mineral exploration is not (as it was previously) that they understand the complexities of relationships between geology and gravity and magnetic fields, but that they can manage the mechanics of running software programs, with responsibility for problem solving progressively ceded to the computer. Furthermore, creation of geological models from geophysical data is currently in danger of being switched to 'automatic' mode by adoption of artificial intelligence (AI) that places more import on its own rules than in the laws of physics. Hopefully this book, in focussing on practical aspects of the application of magnetisation and magnetic field studies in mineral exploration will support more interpretively guided mineral discoveries.

The value of magnetic field data is not as a commodity but in the information it contains. The passage from magnetic field data to an understanding of geology and mineralisation is complicated. The study of geology is largely based on the concept of uniformitarianism – that geology results from processes consistent across the globe and across time. However, each geological system is unique with long and complex sequences of events influencing and modifying each other. Furthermore, in many cases only a small part of a geological system is known from exposure or drill intersection. The search for ore deposits is especially difficult as these are, almost by definition, unusual systems. Throughout this book we repeatedly affirm that quantitative information (such as estimates of depth or magnetisation direction) is only recovered with confidence from magnetic field data in favourable locations where compact magnetisation generates distinctive local curvature in the magnetic field. We define these locations, the data they are characterised by and the magnetisations that give rise to them as 'sweet-spots'. This terminology has not been widely used previously because limits on computational size and speed restricted inversions to only these selected features. With massive advances in computational power it is now feasible to generate large models of the complete subsurface, but as a consequence we now have unfortunate and incorrect acceptance of these models as continuous and reliable three-dimensional maps of physical property values. Geophysicists would prefer this to be true, as would exploration managers, all other consumers of the models and geophysical software developers. It is an 'inconvenient truth' and is not a universally welcomed message that only selective parts of the magnetic field support meaningful inversion. Acceptance of these models also introduces the associated implication that magnetic fields continuously propagate information about their source magnetisation to whatever elevation they are measured at or upward continued to. Previously this was well understood to not be the case, with references to 'distal' and 'proximal' fields as a classification of the level of information in magnetic field data. Unfortunately those terms have fallen out of regular use.

Image processing and enhancement of medium- to high-resolution aeromagnetic surveys has been remarkably successful in support of qualitative geological interpretation and mapping (Isles and Rankin 2013). This does not, however, mean that those same geological features can necessarily be reliably recovered from a three-dimensional inversion model. The success across Australia of geological mapping from magnetic field imagery is in part because of focus on the shallowest substantial magnetisations that are typically at or just beneath the basement unconformity. At greater depths the reliability of magnetic models rapidly dissipates, except in those few windows where there are no significant overlying magnetisations. The central and base sections of a magnetisation are difficult regions to investigate because they lie beneath shallower sections of magnetisation. Obscuring by shallower magnetisation causes much greater loss of reliability for the deeper sections of a magnetisation model than the (already considerable) attenuation of magnetic field signal with depth.

1.1 MAGNETISATION STUDIES IN MINERAL EXPLORATION

The two key applications of rock magnetic and palaeomagnetic studies to mineral exploration are as a tool to investigate the process of mineralisation and to help constrain magnetic field interpretation.

In Australia drill core obtained in mineral exploration programs constitutes a large proportion of the material available for petrophysical studies. Until recently, core from boreholes drilled in short-lived exploration programs was commonly discarded together with its metadata at the end of unsuccessful exploration projects. Fortunately, there is now systematic retention and documenting of core by State and Territory Geological Surveys with internet access to the metadata. However, there is still a backlog of petrophysics measurements on the cores, many of which are unoriented. Systematic growth of data will progressively increase regional knowledge of petrophysical properties, including magnetic susceptibility and remanent magnetisation, and better reveal linkages between those properties and geology, mineralogy and mineralisation. Measured magnetisation values help to constrain magnetic field inversions that extend mapping away from the boreholes and the linkages of magnetisation to mineralogy, alteration and mineralisation support more confident transformation of magnetisation models to geological models.

1.1.1 Ferromagnetism

Magnetisation is a vector field description of the density of magnetic dipole moments in a material. Ferromagnetic magnetisation is characterised by its high strength and a behaviour known as hysteresis, in which self-sustaining magnetisation persists after an applied magnetic field is removed. In consequence, ferromagnetic minerals carry both a component of magnetisation induced in the presently applied field and a 'remanent' component acquired in their previous history. Ferromagnetism is an ordering effect and temperature disorders, preventing magnetisation above a critical temperature for each ferromagnetic mineral, known as its Curie point (580°C for magnetite). Basic igneous rocks are intruded at 1,200° to 1,400° and solidify above their Curie point. As an igneous rock cools through its Curie point it becomes ferromagnetic, but each grain according to its size, shape, chemistry and crystallography may have a short relaxation time within which magnetisation resets. At some temperature below the Curie point, referred to as its blocking temperature, the relaxation time of each grain increases abruptly to periods of geological extent. The population of blocking temperatures in a rock determines the history with which it acquires thermoremanent magnetisation (TRM) on cooling and has it reset by any subsequent reheating, and the vector sum of remanent magnetisations of all ferromagnetic grains in a rock determines its bulk remanent magnetisation (natural remanent magnetisation or NRM).

Within a ferromagnetic mineral grain the space across which a consistently directed magnetic ordering extends is known as a domain. Large ferromagnetic grains optimise their magnetisation energy by arrangement into domains separated from each other by walls (in some cases pinned at crystallographic imperfections) and these grains are known as multi-domain (MD). Magnetisations of MD grains are relatively easily reset by movement of the domain walls and in many cases carry 'viscous' remanent magnetisation (VRM) acquired at low temperatures in the recent geomagnetic field. Grains too small to support an internal domain wall are known as single-domain (s.d.). s.d. grains carry extremely stable remanent magnetisations that can persist since the original formation of the rock provided they are not reheated above their blocking temperatures. However, these grains have small volumes and do not generate a strong NRM unless they are present in large numbers. Fortunately, the range of stable magnetisation is considerably extended by elongate pseudo-single domain (PSD) grains that have only a few internal domain walls with limited options for repositioning. In some igneous or metamorphic rocks, magnetite needles exsolved in the cleavage traces of amphiboles and pyroxenes carry stable ('hard') remanent magnetisation while the larger, more visually obvious blobby magnetite grains predominantly carry viscous ('soft') remanent magnetisation. The contribution of different mineral grains to the magnetisation of a rock was investigated in studies such as reported by Dunlop and Özdemir (1997) at a time when magnetic remanence carriers were the key to digital data recording. Newly developed methods of probing magnetisation of individual mineral grains include scanning magnetic microscopy (e.g. Pastore *et al.* 2019) and micromagnetic tomography (Cortés-Ortuño *et al.* 2022).

1.1.2 Dominant ferromagnetic minerals

Magnetic field variations measured in aeromagnetic surveys do not carry diagnostic evidence of the specific ferromagnetic minerals that generate them; however, only a small number of minerals are significant sources of measured magnetic field variations. Magnetite (ferrous) and hematite (ferric) oxides of the titanomagnetite and titanohematite series respectively as shown in Fig. 1.1 carry many rock magnetisations. These minerals are solid solutions at high temperatures, but at lower temperatures exsolution occurs together with oxidation of titanomagnetites, creating complex magnetisations (Robinson *et al.* 2002; Kasama *et al.* 2004). In a study of the Iron Knob magnetic field anomaly in the Gawler Craton of South Australia extreme remanent magnetisations are associated with fine intergrowths of magnetite and maghemite in hematite that may be an analogue for strong magnetisations in Martian rocks (Schmidt *et al.* 2007).

The titanomagnetite series is a widely distributed common constituent of many igneous, metamorphic and sedimentary rocks. Titanohematites are also widely distributed (in some cases from oxidation of titanomagnetite) but typically have weaker magnetisations. In its monoclinic form the iron sulphide pyrrhotite is also strongly magnetic (with magnetisation intensities similar to magnetite) but pyrrhotite is only weakly magnetic or non-magnetic in its hexagonal form. Pyrrhotite is also

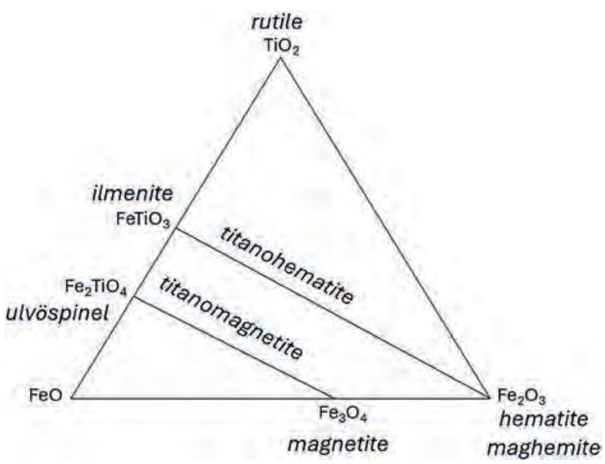

Fig. 1.1. Major iron and iron-titanium oxide ferromagnetic minerals.

more restricted in its occurrence than magnetite, mostly in basic or ultrabasic rocks (in some cases associated with sulphide mineralisation), in contact metamorphic aureoles or in shales created in reducing conditions.

Maghemite is a strongly magnetic iron oxide, in many cases produced at surface, such as in grass fires (Löhr *et al.* 2017). In Australia there are many arid or semi-arid regions where maghemite is widespread in the regolith and gives rise to extensive, sharp variations of tens to hundreds of nanoTeslas (nT) in aeromagnetic data, including dendritic patterns over drainage and paleodrainage systems.

1.1.3 Induced and remanent magnetisations

All ferromagnetic materials carry both induced and remanent magnetisations, but their relative strengths as defined by the Koenigsberger ratio (the ratio of remanent to induced magnetisation) are highly variable and poorly predictable. The Koenigsberger ratio cannot be determined from magnetic field data alone and this scalar measure is insufficient to describe the vector relationship between induced and remanent magnetisation that determines the magnetic field expression of magnetisation (see Chapter 5). For a Koenigsberger ratio of 1, remanent magnetisation parallel to the induced magnetisation doubles the resultant magnetisation, while remanent magnetisation anti-parallel to the induced magnetisation gives a resultant magnetisation of zero intensity. As shown in Fig. 1.2A, the influence of remanent magnetisation differently directed to the geomagnetic field is more fully specified if the Koenigsberger ratio is supplemented with the apparent rotation angle (ARRA) that measures the difference between induced and resultant magnetisation directions (Foss 2017). In favourable situations this angle can be estimated directly from magnetic field data. Figure 1.2B shows the stereographic projection (a projection from unit vectors on a sphere to a horizontal plane) of induced, remanent and resultant magnetisation. The great circle plots the plane in which these three vectors lie, with the intermediate position of the resultant direction determined by the Koenigsberger ratio.

Remanent magnetisation is often and unjustifiably neglected as a contribution to magnetic field anomalies. All ferromagnetism includes remanence contributions, and magnetic field inversions using only magnetic susceptibility values are invalid unless specifically justified by extensive measurement of low Koenigsberger ratios. For inversions performed using only magnetic susceptibility, recovered values should be referred to as apparent susceptibility, allowing that part of that magnetisation may be remanent rather than induced. Furthermore, susceptibility and magnetisation values derived from magnetic field inversion are strictly contrasts rather than absolute values. They are also subject to uncertainty linked with corresponding uncertainty of the magnetisation volumes. Estimates of total susceptibility or magnetisation (magnetic moment) contrasts derived from magnetic field inversion are more reliable than individual estimates of susceptibility, magnetisation or volume.

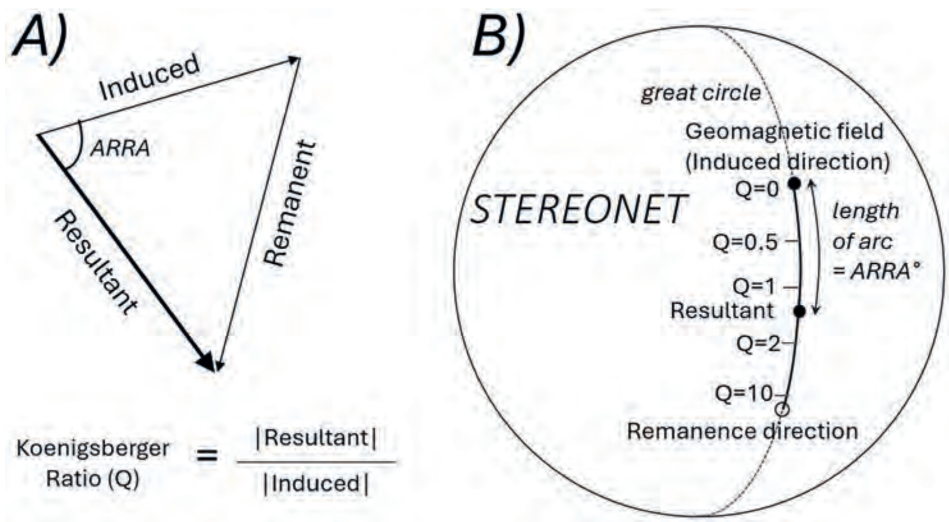

Fig. 1.2. A) coplanar induced, remanent and resultant magnetisation vectors with the Apparent Resultant Rotation Angle, B) Stereonet projection of the geomagnetic field, remanence and resultant magnetisation directions.

Magnetic field anomalies can be inverted with a free magnetisation direction to provide simultaneous estimates of the spatial distribution and resultant magnetisation, but inversion cannot resolve resultant magnetisation into its component parts without independent knowledge of any one of: magnetic susceptibility, Koenigsberger ratio or remanent magnetisation direction. The results of any inversion that limits magnetisation to the present field direction should be confirmed by inversion allowing the magnetisation to have a free direction. If assumption of magnetisation parallel to the field is correct then inversion allowing a free magnetisation direction should confirm that.

For a compact magnetic field variation, inversion provides a reliable estimate of only the mean magnetisation direction. Various inversion methodologies force assumption of a homogeneous magnetisation or allow spatial variation of magnetisation direction, but there is little or no justification to assert that inversion supports either internal distribution. Provided a magnetic field variation is reliably separated from overlapping fields, it is commonly possible to recover estimates of the (contrast) resultant magnetisation direction more reliably than the (contrast) resultant magnetisation intensity.

A major reason why many magnetic field interpretations are made with use of magnetic susceptibility measurements only is the difficulty and expense of remanent magnetisation measurements. Rock magnetic and palaeomagnetic measurements are generally made in specially equipped petrophysical laboratories and the results may not be available at the time they would be needed for input to an active exploration program. An exception is the portable Qmeter (Schmidt and Lackie 2014; Schmidt 2015) that can measure induced and remanent magnetisations in a core shed or at a drill rig for rapid turn-around in magnetic field modelling or inversion. A comprehensive review of the wide range of methods available to determine magnetisation direction is provided by Clark (2014).

1.1.4 Self-demagnetisation

A magnetisation does not sit directly in the background field but in a modification of that field by its own internal field. This influence is termed 'self-demagnetisation' because the internal magnetic field is reverse to the applied field and acts to weaken it and reduce the effective induced magnetisation. At low magnetic susceptibilities the internal field is weak compared to the primary field and can be ignored. At magnetic susceptibilities of ~0.1 SI self-demagnetisation effects become significant, and at susceptibilities greater than 0.4 SI it is essential to incorporate self-demagnetisation effects in any magnetic field modelling. Self-demagnetisation acts to rotate the induced magnetisation direction towards the plane of elongation of a body. At high magnetic susceptibilities, independent constraints become critical to modelling and inversion because the relationship between magnetic susceptibility and the external magnetic anomaly amplitude is highly non-linear. Analytic solution for self-demagnetisation only exists for spherical and ellipsoidal bodies. For sources with sharp edges, corners or internal inhomogeneity there are only iterative approximations that become less reliable with increasing magnetic susceptibility. Iterative computation using equivalent source arrays of dipoles (Purss and Cull 2005) supports computation of self-demagnetisation effects both within a magnetised body and within assemblages of closely grouped bodies.

1.1.5 Anisotropy of magnetic susceptibility

Anisotropy of magnetic susceptibility (AMS) in ferromagnetic materials arises from a combination of crystallographic and shape effects. AMS measurements of oriented samples provide rock fabric information that reveal details of the deposition, intrusion or deformation of those rocks (Hrouda 1982, 2007). AMS also influences the external magnetic field of the induced magnetisation (Biedermann and McEnroe 2017). AMS is described by a symmetric, traceless 3x3 tensor. In extreme cases (such as some banded iron formations) what would otherwise be consistent magnetisation within a folded sheet-like unit gives rise to considerable along-strike variation in its magnetic field expression due to its variable orientation with respect to the inducing field. The differential ease of induction of AMS causes rotation of the induced magnetisation away from the external field direction and towards the 'easy' magnetisation direction. AMS properties known from direct measurement can be incorporated in forward modelling of induced magnetisation but (without considerable independent constraints on other parameters) it is not feasible to ask inversion of magnetic field data to find unknown AMS properties.

1.1.6 Spurious magnetisations

One of the objectives of measuring induced and remanent magnetisations is to help constrain magnetic field interpretation. However, some measured rock magnetisations can give misleading results. Measurement of induced or remanent magnetisation of outcropping rocks may record unrepresentative results from a veneer of weathered surface material even where that weathering is not obvious visually. Conversely, rocks at the site of a lightning strike can display sharp and irregular increase in intensity of remanent magnetisation by several orders of magnitude through acquisition of isothermal remanent magnetisation (IRM). Drill-core can carry magnetisations induced by the drilling and IRM acquired when geologists use a pencil magnet to search for magnetic minerals. Some rocks have particularly soft magnetisations, with VRM components acquired over periods as short as days or hours. This can be detected by storing the samples in a known orientation for a short time before remeasuring their NRM to detect if it has changed. Other samples with even less stable remanent magnetisation may be super-paramagnetic and remagnetise during measurement, but this is readily detected by monitoring the measurement statistics.

Another form of spurious magnetisation arises from misreported units, especially of susceptibility. Magnetic susceptibility is unfortunately defined differently in the cgs and SI systems, giving rise to a difference of 4π (just over 12) between values even though in both cases the units are dimensionless. Magnetic susceptibility is the physical property most measured by geoscientists in the field, using convenient hand-held meters. To accommodate users working in either system, many meters have switches between cgs and SI measurement (with a physical switch on older meters and a software selection on newer meters). Digital output of the newer meters records the metadata of which scale is in use and this information must be retained when transferring data between spreadsheets. Values measured with older meters are of uncertain value unless they have been carefully documented. Neglect of remanent magnetisation in specifying magnetisation in forward or inverse magnetic field modelling is also a form of spurious magnetisation as magnetic susceptibility values alone misrepresent the true magnetisation, even if that magnetisation is parallel to the local field.

1.2 MAGNETIC FIELDS

Magnetic fields are explained by potential field theory as described in many publications (e.g. MacMillan 1930; Kellogg 1967; Blakely 1995). Magnetic potential is the integral of work done to bring a reference pole from infinity to a point and is independent of the track taken. Points of equipotential define a surface and the magnetic field vector at a point is perpendicular to that surface with strength proportional to the potential gradient. The magnetic field can be described as a vector of specified strength and direction (with direction generally measured as a declination angle in the horizontal plane and an inclination angle in the vertical plane) or alternatively as three orthogonal vector components (e.g. east, north and vertical). The magnetic field is piecewise-continuous and smoothly differentiable. In exploration geophysics many measurements of the magnetic field quote only its strength (the total magnetic intensity or TMI) but this is the amplitude of a vector rather than a scalar property.

Some magnetic field studies focus on gradients of the field, either measured or derived by differentiation of field data. For magnetic fields defined by high precision measurements close to each other and of wide extent, a single description of the field carries all the information in the field and any one description is sufficient to derive another (except for indefinite integrals in transforming from gradients to fields). Conversely, if the field is undersampled (e.g. along a single flightline or in a borehole) multi-channel measurements such as different components, tensor gradients or field component and gradient combinations carry more information than single-channel measurements and partially compensate for that restricted sampling. Gradients are an enhancement or 'sharpening' transform relative to the field description and preferentially express nearby sources but they also have more demanding sampling requirements than for the field (Reid 1980).

The three orthogonal gradients of the three orthogonal field components define the gradient tensor. This tensor is symmetric and traceless and is completely defined by one set of off-diagonal terms and two of the three principal elements. The gradient tensor can be directly measured, for instance by low temperature SQUIDs (Schiffler *et al.* 2014), high temperature SQUIDs (Schmidt *et al.* 2004) or diamond nitrogen vacancy sensors (Kuwahata *et al.* 2020). The gradient tensor can also be derived by combination of three orthogonal phase transforms of a TMI grid and then orthogonal gradient transforms of those field components. The relative advantages of direct gradient measurement or transform of TMI data depends on fidelities of both gradient and field measurements, survey line spacing and the proximity and distribution of the magnetisations.

Magnetic fields are additive. The field of a complex distribution of magnetisation can be approximated by summing fields of a suitable array of magnetisation elements – either dipoles or rectangular voxets, or of parametric model bodies such as rectangular prisms, sheets or pipes. In an array of sources, each sits in the external field of the others. However, this consideration is almost never required as the external field of adjacent magnetisations is in almost all cases substantially weaker than the Earth's field. Therefore, it is generally sufficient to sum the independent fields of each source.

1.2.1 The magnetic field of the Earth

Magnetic fields investigated for geological mapping or mineral exploration are samples of the Earth's magnetic field. There are three major contributions to this field; fields generated by current flow in the fluid outer core, ferromagnetic magnetisations in the Earth's crust where temperatures are below Curie point isotherms and fields generated by movement of charged particles in the free space above the Earth. The geomagnetic dynamo is the most prominent contribution and gives the field its major form of an axial dipole approximately aligned with the Earth's rotation axis. Local irregularities in the core field are believed to arise from vortices below the core/mantle boundary. These irregularities grow, die and migrate over periods of hundreds to thousands of years. A key factor of the geomagnetic dynamo field is that it has reversed polarity on multiple occasions, possibly following instances of high symmetry in current flow within the core that reduces the amplitude of the dominant dipole component. The time-average approximation of the geomagnetic field to that of an axial dipole is the basis for latitude estimation in paleomagnetic studies. Across the Earth there is a network of geomagnetic observatories, some of which have provided continuous records over centuries and from which long-term (in the human reference frame) field variations can be tracked. The level of detailed and reliable magnetic field data acquisition is expanding across the Earth to meet increasing needs for geological mapping, mineral exploration, directional drilling and military applications. The growing resource of aeromagnetic data worldwide is also supplemented with satellite data, particularly from the Eusropean Space Agency (ESA) SWARM mission.

The International Geomagnetic Reference Field (IGRF) is a time-varying description of the Earth's magnetic field developed by the International Association of Geomagnetism and Aeronomy (IAGA). Several online tools are available to compute the strength, components, direction and rate of change of the field at any point on the Earth for a specified date and elevation. The 13th generation field is described and defined by Alken *et al.* (2021). The difference in amplitude from over 60,000 nT at the poles to less than 30,000 nT in some equatorial regions (Fig. 1.3A) is broadly consistent with the factor of 2 variation between Gauss-A and Gauss-B positions of a dipole field. Steepening of inclination towards the poles (Fig. 1.3B) that is highly significant for geophysical exploration projects at different latitudes is also broadly consistent with an axial dipole model.

The principal consequence of making TMI measurements in the Earth's magnetic field are that the expression of secondary anomalous fields is strongly influenced by their vector addition with the dominant background field. In the steep geomagnetic inclinations at high latitudes the vertical geomagnetic field component dominates and orthogonal horizontal components in the secondary field contribute little to TMI. In the low geomagnetic inclinations of equatorial latitudes the horizontal northerly-directed geomagnetic field component dominates and only secondary field components parallel or anti-parallel to that contribute significantly to TMI. A further inclination-dependant difference is that the secondary field above an induced magnetisation is parallel to the geomagnetic field in a vertical inclination field, giving rise to predominantly positive TMI anomalies, but is anti-parallel to it in a horizontal inclination field, giving rise to predominantly negative TMI anomalies, as shown in Fig. 1.4. The reduction to pole (RTP) transform seeks to reduce the complexity in relative positioning of a magnetisation and the peak of its TMI anomaly in non-vertical geomagnetic inclinations by a phase transform of both the magnetic field component and the magnetisation. The standard RTP transform assumes that magnetisation is parallel to the geomagnetic field and this transform is invalidated if the magnetisation is differently directed (see Chapter 5). The RTP transform is also unstable if applied to data measured in particularly low geomagnetic inclinations. The phase transform of TMI to vertical component (B_z) data also suffers instabilities in low inclination fields but nevertheless B_z and its vertical derivative $B_{z,z}$ provide considerable advantage in magnetic field analysis (see Chapter 9) without the dependence on magnetisation direction of the RTP transform.

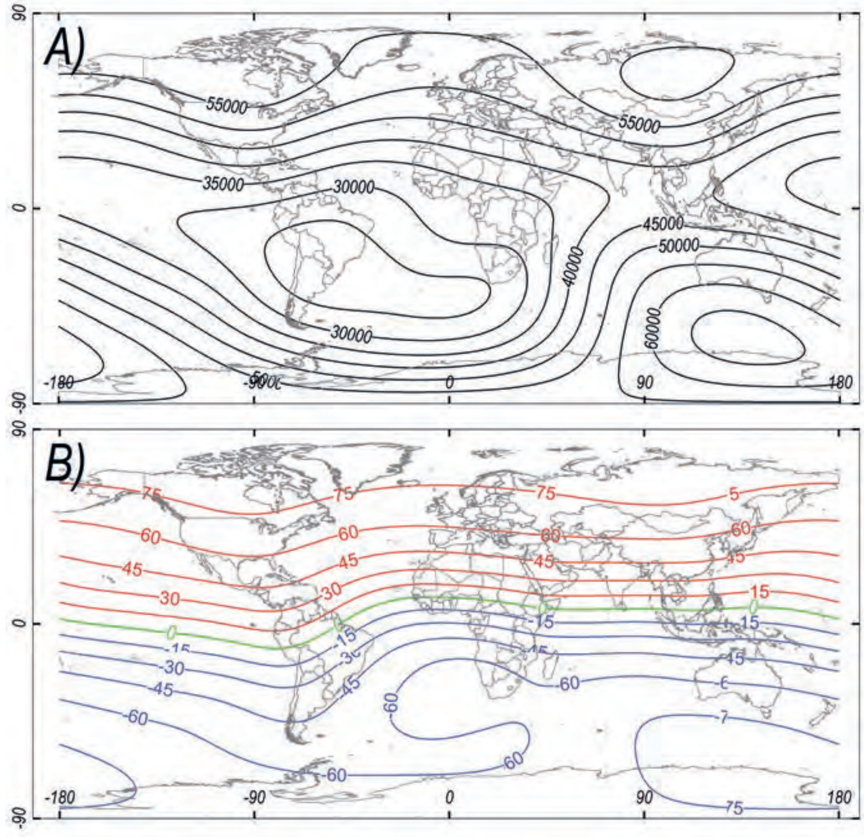

Fig. 1.3. A) Contours of IGRF intensity (nT) and B) contours of inclination of the IGRF (degrees).

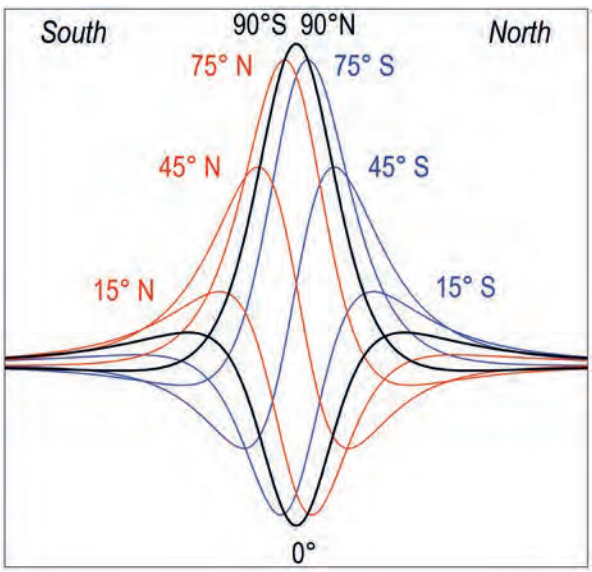

Fig. 1.4. South to north TMI profiles at different geomagnetic inclinations over dipoles with field-parallel magnetisation.

The vertical component of the geomagnetic field is directed downwards (by convention positive) in the northern hemisphere and upwards (negative) in the southern hemisphere. The considerable latitude variation of TMI anomalies generated by field-parallel magnetisations is highlighted in Fig. 1.4. Plotted in black, anomalies in both vertical (± 90°) and horizontal (0°) inclinations are symmetric and almost single-signed. The horizontal-inclination TMI curve is predominantly negative and of lower amplitude than the predominantly positive vertical-inclination TMI curve. At intermediate inclinations the anomaly curves are of dual polarity. In the southern hemisphere (the blue curves in Fig. 1.4) the anomaly peak is to the north of magnetisation with a trough to the south, and in the northern hemisphere (the red curves in Fig. 1.3) the anomaly peaks are to the south of the magnetisation with a trough to the north.

1.3 MAGNETIC FIELD DATA

1.3.1 Sufficiency of sampling the field

We only have imperfect samples of the magnetic field and this invariably imposes limitations in the analyses and interpretations we can make according to data resolution, reliability and distribution. In analysis of magnetic field data it is important to always remain alert to this limitation because as data are progressively processed, enhanced, modelled and inverted the outputs become further removed from the original measurements and our understanding of their information limits. Any processing or enhancement only distils information – it does not create it, whereas poorly considered processing can destroy or distort information.

Most magnetic field data acquired for geological mapping and mineral exploration is measured on aeromagnetic surveys. Measurements are much closer along the flightlines than between them and spatial resolution of the data is mostly determined by line spacing. There is also greater continuity in sensor orientation, measurement elevation and subtraction of diurnal variation along lines than across them. Rule-of-thumb sufficiency estimates can be derived from fast Fourier transform (FFT) analysis of the data sampling in both across-line and along-line directions as discussed in Reid's (1980) seminal paper. Importantly, Reid's analysis emphasises the different data requirements for quantitative map interpretation, working with gradient enhancements and modelling or inversion of the data. In steep geomagnetic inclinations there is obvious advantage in setting the flightline direction perpendicular to geological strike and elongation of magnetic features. Low geomagnetic inclinations introduce the complication of strong horizontal directionality of the geomagnetic field and favours a north–south flight line orientation. Mapping magnetic fields of north–south elongated magnetisations at low geomagnetic inclinations is fundamentally problematic. There are polarisation anomalies at the northern and southern terminations of the magnetisations and only weak magnetic field expression across their central section. This problem is only partially alleviated by choice of measurement or transform strategies.

Bifold classification of an area as having or not having aeromagnetic data available is of restricted meaning. Mineral exploration programs are exercises in problem solving and the critical question of any existing aeromagnetic data is whether it is sufficient to contribute to solving the specific challenges of an exploration program. Existing data over an area should always be examined, but if the line spacing is too wide its main value may be to provide input to design of a more detailed survey. Many of the datasets presented in this book are from regional surveys flown at 200 or 400 m line spacing and typically with 8 m along-line spacing. Chapter 2 includes investigation of resolution differences between a survey flown at 400 m and 100 m line spacing.

1.3.2 Magnetic field grids

It is commonly assumed that a magnetic field grid at all points represents the true magnetic field. However, most grid nodes lie off the survey flightlines and their values are substantially influenced by the gridding algorithm that is used. Gridding is not a 'passive' operation – it creates apparent data where there was none initially. Grids are commonly generated at cell sizes of one-quarter or one-fifth of the flightline spacing. This is a compromise between de-sampling of the line data (for a line spacing of 400 m a cell spacing of 80 m is about 10 times the normal measurement spacing) and suppression of short-wavelength artefacts between lines. As shown in Chapter 2, the magnetic field is severely misrepresented by gridding where flightlines are sub-parallel to the field gradients. At present, grid interpolation is generally performed with minimum curvature algorithms. The limitations of grid interpolation are most evident in regions of particularly sharp field curvature that give rise to 'bicycle-chain' or 'string-of-pearls' artefacts. For data with sharp curvature in one direction, anisotropic diffusion algorithms (Naprstek and Smith 2019; Davis 2022) reduce these problems (as discussed in Chapter 2).

1.3.3 Separation of magnetic fields

Magnetic fields are additive. It is simple to combine fields of different sources (as is regularly performed in forward modelling calls of magnetic field modelling or inversion) but there is no reliable method to perform the inverse operation and achieve unique and correct separation of overlapping fields from different sources. In mineral exploration no magnetic field is measured in complete isolation. More distant or much deeper sources add magnetic field variations to that from any shallower magnetisation of interest. However, it may be possible to separate these fields quite effectively in a process termed 'regional-residual separation' utilising their different curvatures. There are various analytic methods to perform this process but regional-residual separation is fundamentally interpretive. Removal of unwanted shorter wavelength field variations due to shallower magnetisations is also based on differences in field curvature and is also interpretive. The most problematic isolation of magnetic fields is between fields of similar curvature from adjacent magnetisations at similar depth. Field separation is also problematic if fields are insufficiently sampled or if the measurements are of insufficient extent. In these cases field separation contributes substantially to errors and uncertainties in modelling, inversion and interpretation.

Vertical derivative anomalies are more compact than field anomalies and have greater range of curvature with source depth. Both these factors assist anomaly separation but place greater requirements on the spacing and resolution of data. Removal of short wavelength field variations can be best achieved from the original line data because in gridding those variations are partially redistributed and their characteristics become less diagnostic. Line-based filters act on the primary data but only access data on the same line. For instance, the vertical derivative computed as an along-line filter is made on the assumption that the horizontal crossline gradient is zero. Fortunately, this is not a limitation as line-based filters can be applied with advantage in inversion provided they are applied identically to both measured and model-computed data channels (as discussed in Chapter 2).

Anomaly separation is particularly important in estimation of magnetisation direction. The symmetry/asymmetry of a magnetic anomaly is a critical expression of the source magnetisation direction that is also influenced by any elongation of body shape or by superposition of other fields across the anomaly or some part of it.

1.3.4 The vector nature of TMI data

Almost all magnetic field surveys for geological mapping and resource exploration measure TMI. As shown in Fig. 1.3A, the IGRF amplitude varies from ~30,000 nT near the equator to more than 60,000 nT close to the poles. Few measured local magnetic field variations have amplitudes greater than 1,000 nT and therefore they do not significantly deflect the local geomagnetic field direction. However, at locations of particularly strong magnetisation (including commercial magnetite deposits) magnetic field variations can be of much higher amplitude, resulting in significant rotation of TMI within those areas. In such cases, measured TMI must be corrected to a consistently directed vector using an iterative scheme (Lourenço and Morrison 1973; Clark 2013) before it can be treated as a potential field. This step is not required for modelling or inversion where TMI is computed at each point from its three individual field components.

In the Earth's magnetic field it is not feasible to accurately measure individual magnetic field vector components that are penalised by their slightest sensor misorientation in the background field. Chapter 11 considers the quite different challenge of making magnetic field measurements in weak magnetic fields away from the Earth. In weak fields, orientation penalties are substantially reduced and conversely there is a problem with TMI measurements because the field orientation is highly variable and poorly predictable. The problem of orientation sensitivity in the strong background field of the Earth is substantially reduced by working with gradients. Background gradients of the Earth's magnetic field are typically much weaker than those of magnetisations of interest sourced at shallow to intermediate depths. Horizontal along-line TMI gradients can be reasonably recovered from aeromagnetic survey data by differencing sequential along-line measurements, and in some surveys horizontal crossline gradients are measured using a pair of wingtip magnetometers. To date, application of these data has been mostly restricted to improved processing of TMI grids with few efforts to exploit the data for modelling and inversion studies. Vertical gradients have also been measured by mounting a pair of vertically displaced TMI sensors on the aircraft tail, but this has had limited success due to the short baseline. Recently, measurements have been extended to the gradient tensor using SQUID detectors (Schmidt *et al.* 2004; Schiffler *et al.* 2014) and diamond nitrogen-vacancy magnetometers (Kuwahata *et al.* 2020). Tensor gradiometer surveys have yet to be adopted in standard aeromagnetic surveying and have mostly found application in the search for small and shallow kimberlite targets in diamond exploration or for unexploded ordnance. For these anomalies defined on only a few flightlines there is significant advantage in multi-channel data, provided the gradients can be measured with sufficient precision. A major challenge to any gradient data, whether derived from direct measurement or transform of field component measurements, is presence of short-wavelength noise from data imperfections and/or platform or near-surface geological magnetisations.

1.3.5 Magnetic field expression of the centres and edges of magnetised bodies

A magnetic field anomaly due to a magnetisation parallel to the inducing field can be simplified with a standard RTP transform (Baranov and Naudy 1964). Using a modified transform, RTP can also be performed for another, known magnetisation direction. Correctly applied RTP transforms peak over or close to the horizontal centre of magnetisation (unless displaced by the disproportionate influence of the shallowest sections of a plunging magnetisation). An alternative approach to locating the centre of magnetisation is to apply a transform such as the total gradient or 'analytic signal' (Nabighian 1972) that approximately locates the centre of a compact magnetisation with reduced influence of its magnetisation direction. The normalised source strength (NSS) transform (Beiki *et al.* 2012) mostly locates the centre of magnetisation more closely but at the cost of greater computational complexity. Both the analytic signal and NSS transforms enhance the field contributions of the shallowest magnetisations.

In the case that a body of magnetisation is wide compared to the elevation at which the field is measured, magnetic fields and their associated gradients change more rapidly towards the edges of magnetisation rather than towards its centre. In a non-vertical geomagnetic field, with magnetisations parallel to the field, there is polarisation over the northern and southern margins with quite different field variations over those two margins and with lower amplitude expression of the eastern and western margins. In a steep geomagnetic field shallow wide sheets of small depth extent with induced magnetisation generate a continuous or near-continuous anomaly peak just within the margin of the magnetisation and a flanking trough just outside it. Steeply dipping edges of wide magnetisations can be approximated located using the peak horizontal or peak total gradient of the RTP field (Blakely and Simpson 1986; Grauch and Cordell 1987; Fedi and Florio 2001). Roest *et al.* (1992) and Wijns *et al.* (2005) developed gradient-based analyses to enhance the expression of magnetisation edges in magnetic field data.

If an upward continuation is applied to magnetic field data before resolving gradients, the gradient peaks migrate in the direction of dip (Archibald *et al.* 1999; Hornby *et al.* 1999) because the upward continuation more heavily weights contributions from the deeper zones of magnetisation relative to the shallower ones. Assistance in analysis of complex gravity and magnetic field variations is provided by an automated vector analysis applied to the gradient maxima, termed 'multiscale edge analysis' or 'worming' (Boschetti *et al.* 2001). The success of this method depends on the nature of the physical property contrasts in the ground and the sufficiency of data coverage. The horizontal gradient transform applied to gravity data or appropriately transformed RTP magnetic data highlights shallow density or magnetisation contrasts respectively. Applying an upward continuation to the gravity or magnetic field data before the horizontal gradient transform preferentially attenuates field variations from the shallowest property contrasts and places greater focus on deeper property contrasts. A series of analyses with increasing upward continuations produces a series of vectors with progressively increased weighting of deeper property variations (although it is not feasible to link analysis at any one continuation height to property contrast at any specific depth).

1.3.6 Spurious magnetic field variations

A sound approach to inspection of new data is to be suspicious of everything and expect errors. Magnetic field data are geolocated and one source of error in the data that might not be obvious in its initial inspection is that it might be incorrectly located. At present, with GPS positioning and use of standard projections there should be little scope for incorrect location, but in Australia historic aeromagnetic data are still being used that was acquired when two projection systems were in common use (AGD66 and WGS84) with differences of ~200 m. This unfortunate situation resulted in frequent mislocation of data and it is by no means certain that all data of that vintage has a correctly attributed projection.

Magnetic field expressions of man-made objects in aeromagnetic data are commonly referred to as 'cultural' anomalies. In some cases these have diagnostic characteristics that reveal their origin but in a survey with many shallow-sourced anomalies there may be several of uncertain origin. We now have unprecedented coverage of surface imagery (including Google Earth) on which a magnetic field image can be overlaid to investigate whether an anomaly of uncertain origin coincides with a man-made feature, although this check does not detect temporary features that may have been present when the aeromagnetic survey was flown but not when the surface imagery was acquired. If a survey is to be flown over a developed area where cultural anomalies are anticipated, surface imagery can be acquired with the survey to evaluate possible cultural anomalies (as is conveniently done for small area drone surveys).

Most evaluation and interpretation of magnetic field data is performed using grid imagery. One of the more common artefacts encountered in grid data are flightline level shifts that appear as linear features in the flightline direction. Micro-levelling attenuates these features but may leave subtle, longer wavelength features that can be confused with geological signal. Survey grids can also include point anomalies due to gridding of any unremoved spikes in the line data (particularly at line terminations). Grids should be tightly clipped to the extent of input data to avoid spurious apparent coverage of unsurveyed areas where the grid is an extrapolation of the gridding algorithm rather than interpolation of measurements. Magnetic field analysis and interpretation is generally best optimised on application to individual surveys, but sometimes data are available only as composite grids of multiple surveys and there may be spurious level shifts between surveys or differences in line spacing, line orientation and/or flying height that confuse evaluation of features in the different survey areas. Grid stitching that is performed where there is overlap between adjacent survey grids acts to disguise differences between those surveys, effectively by distorting the data in the area of overlap where the resulting grid may be incompatible with both input grids. The result may be cosmetically more acceptable and support enhancement of the combined grid that would otherwise be distracted by the local disconformities at grids margins, but a mosaic of grids can mislead interpretation of the data.

1.3.7 Static and dynamic magnetic fields

Conventional magnetic field surveys are classified as 'static' because they aim to define the magnetic field at one instant of time through elimination of time variations of the field over the duration of the survey (using diurnal corrections made at a fixed base station). 'Dynamic' surveys with a time series of measurements at each survey station should provide capabilities to map spatial variation in time variations of the field (Goldstein and Ward 1966; Clark *et al.* 1998). These field variations due only to changes in induced magnetisation can be analysed or inverted with the advantage of the known magnetisation direction. Dynamic survey procedures are challenging because the amplitude of 'quiet day' diurnal variation that induces the dynamic anomaly is only of the order of 1,000th of the total geomagnetic field that induces the conventional static anomaly, and because each station requires multiple measurements in highly repeatable position and orientation at different times. However, if a reliable model can be generated from inversion of the dynamic anomaly then the static magnetic anomaly can be subsequently resolved into induced and remanent magnetisation components using that spatial model. We now have SQUID magnetometers and gradiometers of sufficient precision to attempt these surveys on the ground (Foss *et al.* 2019). The time required for multiple repeat measurements is likely to limit surveys to a small number of stations. However, the method may be useful for investigation of elongate anomalies over sheet magnetisations for which separation of structural dip and inclination of magnetisation is particularly uncertain in conventional magnetic field analysis. Potentially, high-resolution inversion of anomalies measured on conventional aeromagnetic surveys flown decades apart might support a dynamic field analysis but this would require

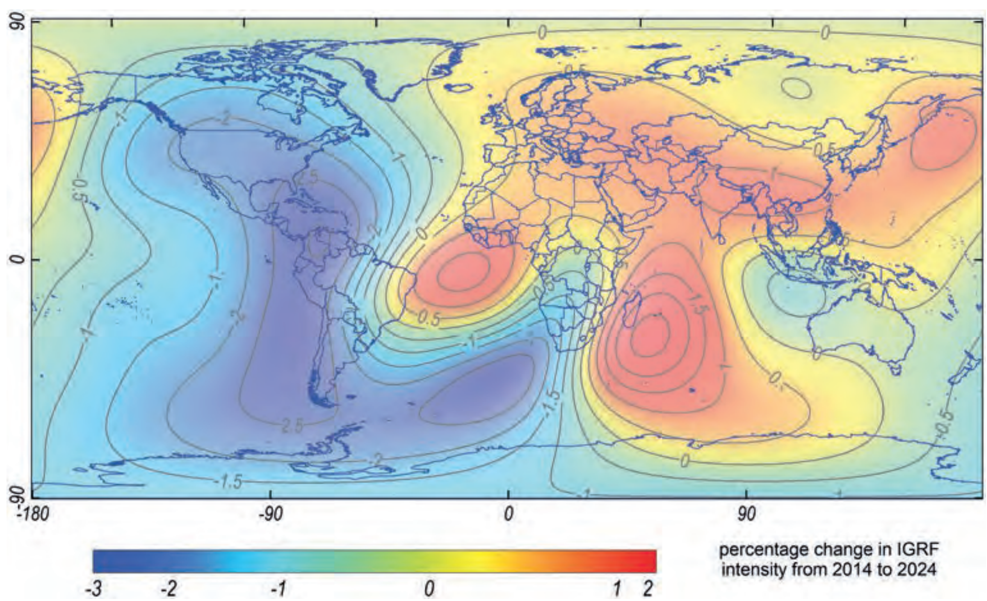

Fig. 1.5. Percentage change in IGRF Intensity over the period 2014.5 to 2024.5.

extreme measurement precision and substantial differences in the geomagnetic field between the different survey dates. Figure 1.5 shows that high-amplitude decade-long variations in the field occur in a few (mostly offshore) regions across the globe, with onshore TMI intensity variations over the last 10 years mostly less than 1% of the total field strength (increase or decrease in the field strength are equally suitable for dynamic field analysis). At present, the only convincing detection of time differences in naturally sourced magnetic anomalies are from surveys flown above active volcanoes (Koyama *et al.* 2013) where magnetisation differences may be due to physical movement of magnetisation and/or abrupt temperature variations.

1.3.8 Relationships between magnetic and gravity fields

Rock magnetism is dominated by ferromagnetic minerals that typically constitute only a few per cent of a rock or less. In contrast, the density of a rock is determined by all its components, including fluid-filled pore spaces. Many observed variations in the gravity field are generated by density contrasts of the order of 10% of total density and the issue of density contrast is foremost in consideration for interpretation of gravity data. For many interpreted magnetic field variations the magnetisation contrasts are almost the same as the absolute magnetisation values and the concept of contrast is commonly neglected. Furthermore, magnetisation contrasts are vector rather than just scalar contrasts.

Gravity and magnetic fields are governed by common mathematical laws of potential field theory (Blakely 1995) with the dipole magnetic field an order of curvature higher than the monopole gravity field. As determined by Poisson's theorem, for a constant relationship between density and magnetisation, the vertical gradient of gravity $g_{z,z}$ is directly proportional to the vertical magnetic field due to vertical magnetisation (the RTP of TMI). With an assumed or known magnetisation direction, gravity fields can be expressed as equivalent magnetic fields using the pseudomagnetic transform (Blakely 1995). Conversely, magnetic fields can be expressed as equivalent gravity fields using the pseudogravity transform (Baranov 1957). Complex density and magnetisation variations invalidate the basic assumptions of these transforms and only in quite rare circumstances do pseudogravity or pseudomagnetic transforms approximate to the true gravity and magnetic fields. Interpretation from visual evaluation of large gravity and magnetic images is challenging because of the complexity and different dynamic ranges of the individual datasets. Figure 1.6 shows Bouguer gravity and TMI images of the Barton area of the southern Gawler Craton in South Australia (Foss *et al.* 2019a). The Bouguer gravity grid is derived from station spacings of 8 km over the west and centre of the area and 2 km over eastern part of the area, and the magnetic field is measured on east–west flightlines at 200 m spacing across the complete area. There are clear associations between the TMI and Bouguer gravity grids but direct comparison is challenging because of the complexity of each image.

Figure 1.7 shows vectors developed from multi-scale edge analysis (see section 1.3.5) of both the gravity and magnetic fields. These are independent fields mapped by completely independent data. The gravity data are measured at ground stations and the aeromagnetic field on flightlines at a nominal 80 m ground clearance, yet there are considerable similarities between the vectors derived from the two datasets. Each vector set is extracted from a series of upward continuations. For the lower-level continuations in each set (with signal predominantly sourced in the shallow subsurface) there is a larger number of vectors, including many short vectors. For the higher-level continuations (with signal more strongly sourced from greater depths) only the longer vectors persist. In Fig. 1.7 I have selected gravity vectors from one continuation level (1286 m) and magnetic vectors from a deeper level (1970 m) to best highlight the correspondence between the two fields. There are many features with near-identical traces in the two data vector sets, revealing that they are generated by geological contrasts with both density and magnetisation expression. Some features have combined expression along segments of their lengths and only gravity or only magnetic expression along other segments. There are also vectors almost perpendicular to each other, where a vector from one set terminates against a vector from the other. There is clearly additional information relating to the geology available from combination of the two geophysical methods.

Combined airborne gravity gradiometer (AGG) and aeromagnetic surveys are flown in mineral exploration programs, but unfortunately cost has to date restricted widespread application of AGG for regional geological mapping. AGG surveys are more appropriate for revealing relationships between gravity and magnetic fields than are aeromagnetic and ground gravity surveys because the measurements are co-located and are of

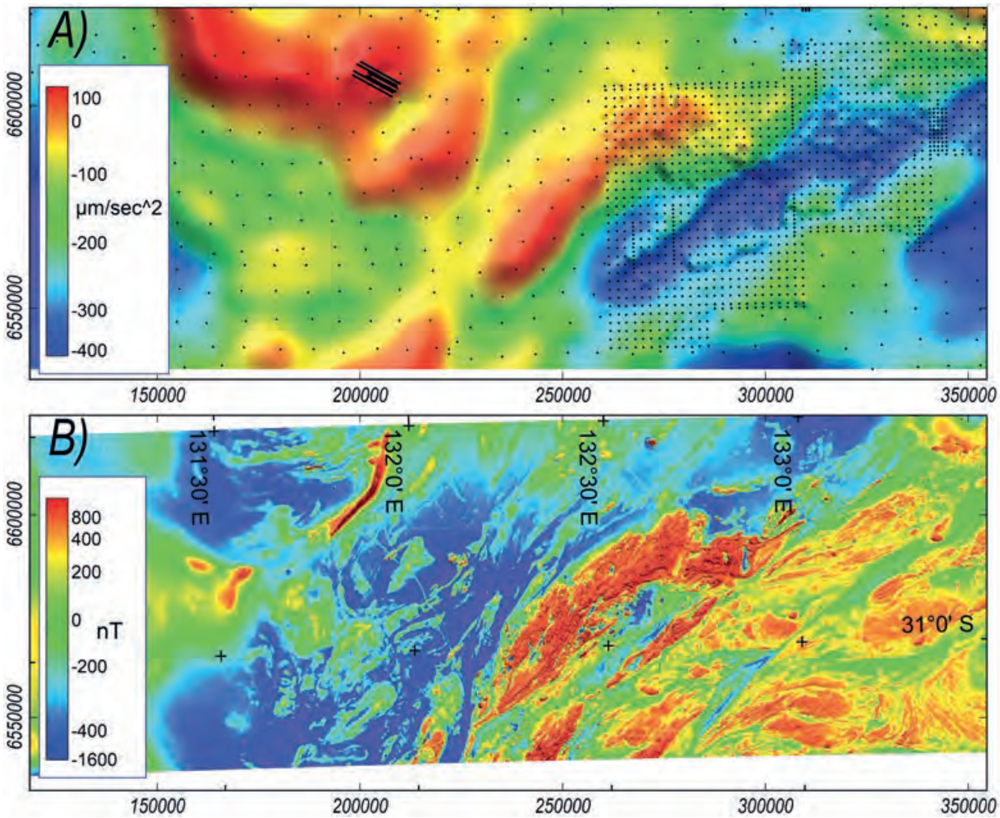

Fig. 1.6. A) Bouguer gravity (reduction density 2670 kg/m^3) and B) RTP of TMI over the Gawler Craton, Barton 4A survey area.

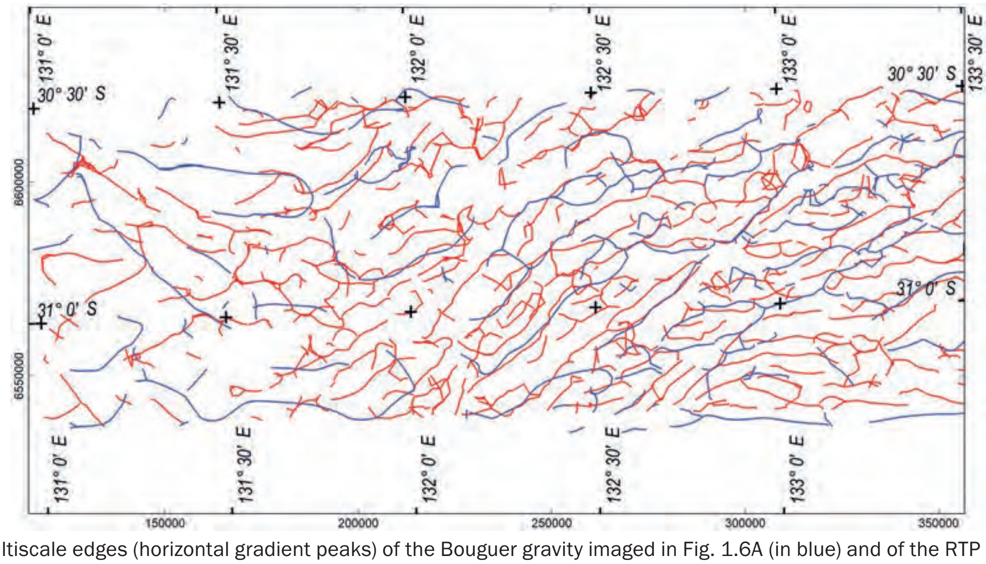

Fig. 1.7. Multiscale edges (horizontal gradient peaks) of the Bouguer gravity imaged in Fig. 1.6A (in blue) and of the RTP of TMI imaged in Fig. 1.6B (in red).

matching curvature expressions of the fields (gravity field gradients and the magnetic field). However, even for combined AGG and aeromagnetic surveys the two datasets in most cases highlight different aspects of the geology. In some areas the most prominent magnetic field variations are of small but shallow magnetisations of only small anomalous mass that may not be detectable or are only weakly evident in the AGG data. Conversely, many bodies large enough to have recognisable expression in the AGG data may either be magnetically bland with little expression in the magnetic field data or have substantial internal magnetisation variations and appear as multiple smaller magnetic sources.

An unusually clear correlation between ground gravity and aeromagnetic anomalies is shown in Fig. 1.8 over a segment of the Gairdner dyke swarm in the Torrens 3B Gawler Craton Airborne Survey (Foss *et al*. 2018) in South Australia. The gravity field is mapped by a 17 km × 18 km survey at a station spacing of 400 m (approximately 2,000 stations). Figure 1.8 shows RTP of TMI contours at a 50 nT interval over an image of the vertical gradient of Bouguer gravity generated by FFT. The strong correlation is because the gravity field is mapped to an unusual degree of detail by the 400 m spaced stations, because the dykes are unusually wide and have large volume, and because the dykes intrude through the crystalline basement into the lower-density overlying siliclastic Pandurra Formation. The density contrast for this shallow section of the dykes may be as high as 500 kg/m^3. Figure 1.9 shows a section of an east–west profile constructed from the 400 m spaced gravity stations. The individual dykes are scarcely recognisable in the gravity (g_z) profile (Track A in Fig. 1.9) although they can be traced in a contoured map view because of their continuity between successive profiles. The dykes are much more easily recognised in the vertical gradient of gravity derived from a grid FFT and sampled back onto the line (Track B in Fig. 1.9). Three prominent anomalies in centre of this track are labelled 'a', 'b' and 'c' in Fig. 1.9B. Track C shows a profile of TMI sampled from the grid at each of the gravity stations. The TMI anomalies are strongly undersampled at the 400 m gravity station spacing, generating sharp, almost single-station anomalies for the western and eastern gravity anomalies 'a' and 'c'. There is only weak TMI expression for the central gravity anomaly 'b'. Track D in Fig. 1.9 shows the TMI profile along the nearest, almost co-located flightline. From the enhanced gravity map image in Fig. 1.8 (and the corresponding but higher-resolution TMI map not shown here) the central gravity anomaly 'b' is two weaker magnetic anomalies (as seen in Fig. 1.9 track D) with magnetic field expression poorly sampled at the gravity stations but with a

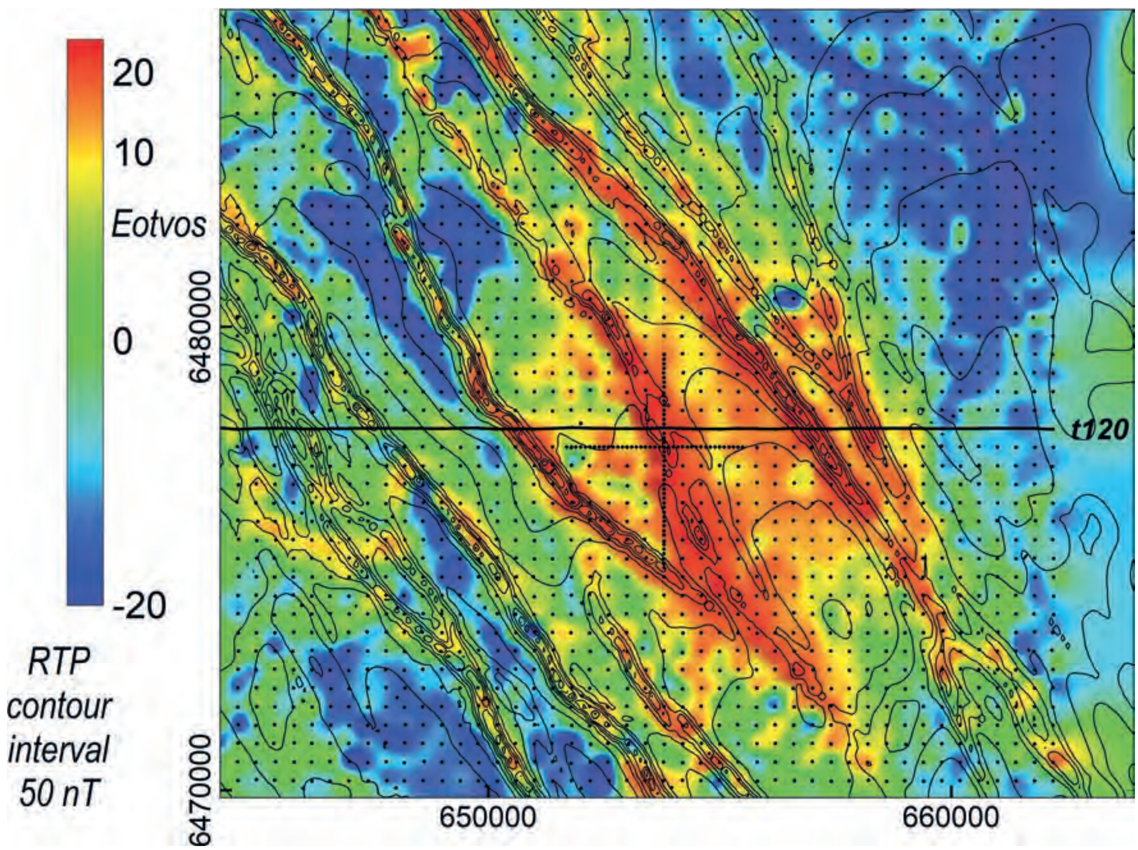

Fig. 1.8. Vertical derivative enhancement of Bouguer gravity as an image and aeromagnetic TMI contours over a part of the Torrens Area 3B of the Gawler Craton Airborne Survey in South Australia. Gravity stations are at 400 m spacing. T120 is an aeromagnetic survey flightline imaged in Fig. 1.9.

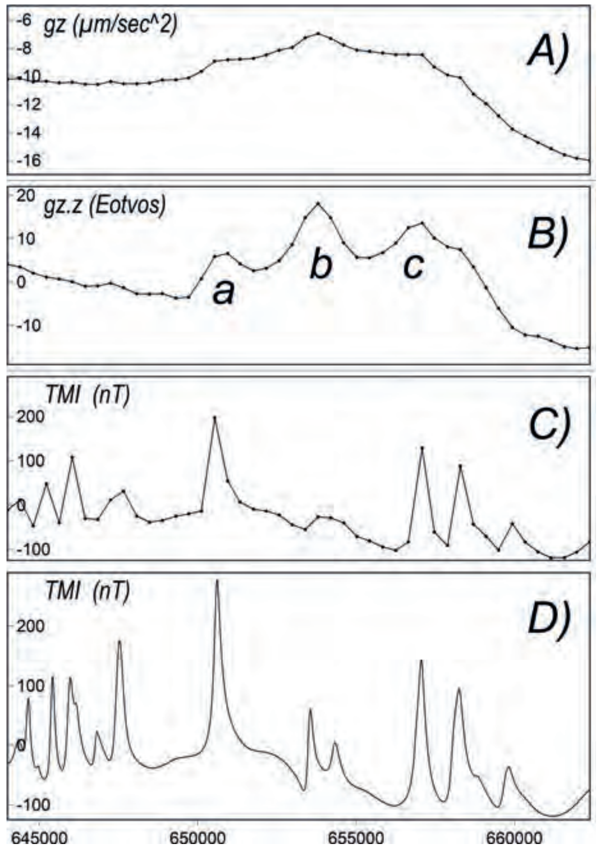

Fig. 1.9. A) ground Bouguer gravity, B) vertical derivative of Bouguer gravity (from a grid FFT), C) TMI sampled at the gravity stations and D) measured TMI along the aeromagnetic flightline T120.

strong combined expression. The considerable difference in resolution between the magnetic field tracks C and D in Fig. 1.9 reveals the major advantage of aeromagnetic data with close point spacing (in this case < 7 m) compared to the wider gravity station spacing.

1.4 MAGNETIC FIELD INVERSION

The objective of magnetic field inversion is to investigate and evaluate the information content of the input data. The lesser achievement of finding a model or a set of models that can match the data can easily be misleading. Most published inversion studies are prefaced with an acknowledgement of the limitations of non-uniqueness but still provide and draw conclusions from models that inadequately represent the range of possible solutions. Non-uniqueness arises from the ability of variation in one or more details of a magnetisation to effectively compensate for variation in others. The fundamental restriction of non-uniqueness is that we cannot know whether an inversion model is a reasonable representation of the true magnetisation in the ground however well it matches the input data. It is therefore not feasible to assign meaningful conventional uncertainty measures to inversion models (if we cannot know the fundamental validity of a model we also cannot constrain it with uncertainty bounds).

Many different challenges arise in day-to-day magnetic field inversion, and the optimised solution of each problem requires a versatile library of different inversion utilities. The key determinants in making the choice about how best to perform an inversion are:

1) what question is to be answered?
2) what is already known about the geology?
3) what data are available?
4) how much time is available to derive a solution?
5) how much exploration of alternatives is required or justified?
6) what inversion resources are available and how can they be optimised for this task?

Non-uniqueness of the inverse problem opens the possibility to such a wide range of solutions that it is invaluable to have a basis of geological knowledge and understanding of the area to be able to hypothesise about the source of a magnetic anomaly and place some limits on the expected distribution of magnetisation. A physicist with no knowledge or understanding of geology can efficiently invert a magnetic field variation to obtain a source magnetisation model, but unless there is basic geological guidance it is unlikely that the model obtained will be geologically feasible. The two most common choices in style of inversion are voxel inversion (the most popular) and parametric inversion. This classification is based on the nature of the models used and the mechanics of how the inversion is performed. Voxel inversion provides much more apparent detail than parametric inversion of the same data but that additional apparent detail is mostly unjustified.

1.4.1 Voxel inversion

The factors to be addressed in voxel inversion are primarily in design of a model objective function that oversees the underdetermined problem of assigning values to a large number of cells (voxets) as well reviewed by Li and Oldenburg (1996). Of particular importance is a depth weighting function to supervise distribution of magnetisation with depth for which the magnetic field provides little definitive assistance. Depth weighting is empirically applied to encourage extension to depth of magnetisations that would otherwise occupy only the shallowest parts of the model. The depth weighting is also generally combined with guidance that variations in magnetisation should maximise smoothness or compactness of magnetisation. These are sound principles for selection of models (just as acceptable as the homogeneous magnetisation assumptions of most parametric modelling) but, as with the parametric model assumptions, there is no *a priori* reason that a geological magnetisation will conform to these assumptions.

Once a voxel inversion scheme has been designed, it is quite straightforward for a user to perform an inversion by following a routine process of defining the architecture of the model (its three-dimensional extents and cell sizes) and submitting the data in an appropriate format. This involves few critical decisions and does not require an expert understanding of the inversion process. Ease of use is a key attraction for voxel inversions. The major step of isolating the field variation to be explained by the model can also be automated and included seamlessly in the inversion process, but field separation is fundamentally non-unique and interpretive. Li and Oldenburg (1998) provide a robust separation method based on prediction from the surrounding field variation that is well suited to automation and simplicity of use. In optimal cases of well-isolated anomalies, most regional-residual separation methodologies should provide very similar output. However, an interpreter should carefully inspect the field data to make an optimum selection for inversion and to develop a strategy to best address issues of anomaly separation. Decisions and findings from that process should be described in any subsequent review and use of the resulting model (possibly including alternative separations). A drawback of a fully automated process is that users of the inversion results are unaware of any issues that may have influenced field separation and thereby the output model.

Each individual rectangular prism of the subsurface magnetisation is specified by its three-dimensional address in the space-filling voxel array, and the summed magnetisations of that array generate the model-computed magnetic field. The prisms may have uniform dimensions, or to lessen computation load, the size and depth-extent of the voxels may increase with depth. A voxel model has the attraction to its users of representing magnetisation throughout the complete subsurface volume, although it is misleading to report values for many parts of the model in which there is no justified confidence.

There are two common representations of voxel models: thresholding the model by displaying only those voxels of magnetisation greater than a selected value, or an isosurface (or isosurfaces) from three-dimensional gridding of the inverted magnetisation. Note that neither of these options clearly displays the magnetisation distribution that matched the anomaly. Both exclude representation of magnetisation below the threshold or isosurface value, and both fail to represent internal inhomogeneity within the displayed magnetisation. Alternative displays are colour-coded model slices along appropriate lines of section that better reveal details of the variation in magnetisation.

Lelièvre and Oldenburg (2009) developed algorithms to allow for inversion of data where magnetisation direction is unknown. Throughout this book many examples are shown to illustrate that magnetisation direction for a compact magnetisation is a bulk property, and that provided the field of a magnetisation can be reasonably separated from other fields, the mean magnetisation direction can be recovered with reasonable confidence (this can be achieved by voxel or parametric inversion); however, there is no analytic justification that spatially variation in magnetisation direction can be reliably recovered from magnetic field data. The concern is not that a model cannot be found but that any model that is found might not be justified. Both voxel and parametric estimates of magnetisation direction are therefore more reliably constrained as single estimates of mean magnetisation direction for each spatially separate feature in the magnetic field (each discrete anomaly or sweet-spot).

1.4.2 Parametric inversion

Parametric inversion has a quite different approach to voxel inversion. With parametric inversion a model is constructed based on interpretive decisions about the feasible distributions of magnetisation required to explain it. A fully space-filling model identical to a voxel inversion could be constructed (with difficulty) by parametric inversion but inclusion of components that are essentially unconstrained by the magnetic field variation is of no advantage. Minimalist models constructed with one source assigned to each discrete magnetic field variation are more easily justified. The forward modelling codes used in parametric inversion are derived for ideal geometries (polyhedral bodies, ellipsoids etc.) of homogeneous magnetisation, but models need not be accepted at this exact level of representation and their magnetisations should only be interpreted as mean values without resolution of internal distribution. Few geological bodies, except for some basalt or dolerite sheets such as dykes, have both homogeneous properties and near-ideal geometries. The most acceptable representation of parametric inversion models is as sets of key statistics, including centre points, approximate horizontal and vertical extents and orientations and total contrast magnetisations (rather than individual magnetisation and volume values).

Parametric inversion is well suited to one-to-one matching between sweet-spots and inversion model bodies. Inversions can address multiple sweet-spots using multiple bodies with advantage if their magnetic fields overlap. However, inversions generally benefit from as tight a focus as feasible. Another aspect of parametric inversion well matched to the sweet-spot approach to magnetic field modelling and interpretation is the strength of parametric modelling in support of model testing and sensitivity studies. Parametric sensitivity tests are performed by offsetting an individual parameter from its value in the global minimum misfit set and repeating inversion with that parameter or parameters held at their offset values to investigate what increase of the misfit statistic this causes, and what adjustments this evokes from the other parameters. Compensation can also be restricted to variation of one other single parameter to investigate more specific cross-correlation between parameters. These tests are most conveniently performed with parametric inversion, but their findings illustrate fundamental aspects of inversion that apply to understanding results of any inversion methodology.

1.5 RELATIONSHIPS BETWEEN MAGNETISATION AND THE MAGNETIC FIELD

The relationship between magnetisation and the magnetic field at first appears a straightforward causative relationship as depicted in the left-hand vertical side of the schematic in Fig. 1.10. It might be thought that this cause-and-effect relationship should be simple to establish. However, this is a complex, non-unique task. The intermediate step in linking an unknown subsurface magnetisation to its remotely sensed expression in the magnetic field is creation of a model or models of the magnetisation (as shown in the other two sides of the triangle in Fig. 1.10). The models may be simple conceptual ideas of what or where the magnetisation is, or specific definitions of magnetisation values and distributions. Until a magnetisation is extensively intersected by drilling or is excavated, we only know it by its model representation. If we already had the model we could verify it by forward computing its magnetic field expression and measuring the field data to test it, but we almost invariably have to work in the opposite direction of first measuring field data and then inverting that data to find a model. From the magnetic field to a model is a one-to-many relationship and ambiguity is widely perceived to be the source of all problems in magnetic field inversion. However, potential field theory places constraints on what we can know from the magnetic field data in much the same way that quantum

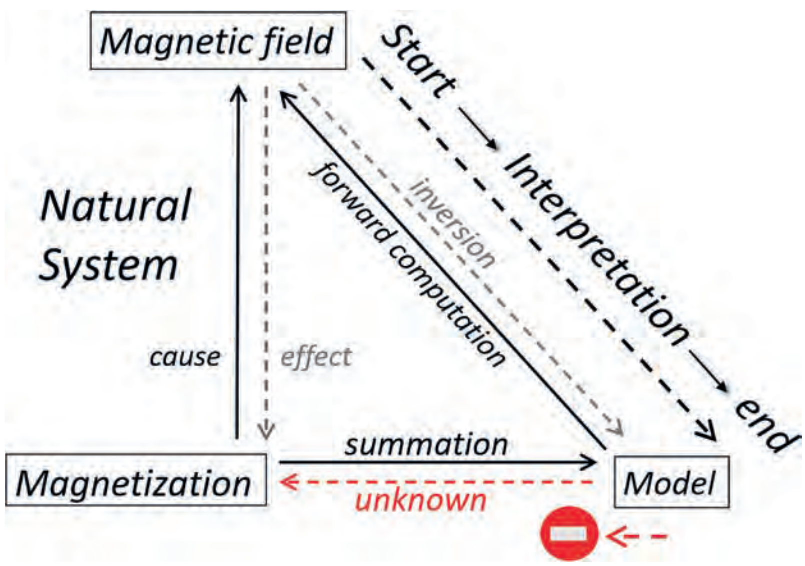

Fig. 1.10. A schematic representation of the relationships between magnetisation, the magnetic field and models.

uncertainty prevents simultaneous knowledge of the position and momentum of a subatomic particle. We should consider that a model obtained by inversion of magnetic field data is a speculation rather than a direct representation of the magnetisation and reclassify the problem to lie mostly between the model and magnetisation as shown in Fig. 1.10 rather than between the model and magnetic field.

Many of the challenges of relating measured magnetic field variations to measured magnetisations depend on scale. Most magnetic susceptibility measurements are made with hand-held susceptibility-meter measurements that sample only a few cubic centimetres of sample and remanent magnetisation is generally known from measurements of a small set of cylindrical plugs of 2.5 cm diameter and 2.5 cm height. Conversely, many magnetic field variations are measured at elevations tens of metres above the Earth's surface and have horizontal extents of tens of metres to kilometres. For even the smallest and shallowest-sourced anomalies we never have direct sampling of more than a very small fraction of the magnetisation that causes the anomaly. This problem is compounded by variability of magnetisation at all scales, within borehole cores and undoubtedly throughout the remainder of the source body that is not tested by drilling. Extensive programs of drilling and measurement of magnetic susceptibility and remanent magnetisation to directly relate geology or mineralisation with magnetisation are rarely feasible. The challenge can be divided into two parts: the challenge of representing the true magnetisation distribution with a model and the challenge of resolving a model from the magnetic field data.

1.5.1 The relationship between magnetisations and their models

Subsurface magnetisation can be envisaged as the true (voxel) distribution that is a digitisation of the magnetisation at regular horizontal and vertical spacing. The challenge of either voxel or parametric models is to best and most reliably represent this distribution of magnetisation. There are different geologies that variously favour representation by sharp discontinuities in magnetisation across individual body margins of parametric models or by the smooth variations imposed on most voxel models. For estimation of the detail of depth to the top of magnetisation, specific shape assumptions of parametric bodies with horizontal tops and sharp edges are required (or at a minimum these can be substituted by shape-related 'structural indices'). If a magnetisation is diffuse and of gradual spatial variation (as assumed or allowed in many voxel inversions) it is not possible to reliably invert for depth to its top. Voxel models are favoured by geologists in part because of their irregular shape and variation in intensity of magnetisation that appears to mimic variation expected of most geological systems. However, it is specifically this level of detail that is the least reliable aspect of the models and is an embellishment of the information that can reliably be recovered from a model. Neither can the implied homogeneity of parametric models be justified. A model of subsurface magnetisation is best envisaged as a set of statistics that summarise a distribution that cannot be known in detail from its magnetic field expression. The set of statistics is necessarily sparser for deeper parts of the model or for models derived from measurements at higher elevation.

To highlight the range of models that can explain a magnetisation I show multiple inversions of a sweet-spot measured in the Coonabarabran Survey (P1290) in northwest New South Wales. Figure 1.11A shows the TMI image of a section of the survey that was flown for the Geological Survey of New South Wales in 2017, on east–west flightlines at 250 m spacing and 60 m ground clearance. Figure 1.11B shows the detail of a discrete anomaly recorded in the survey. This concentration of magnetisation and the aeromagnetic measurements that define its magnetic field expression constitute a sweet-spot from which magnetisation details can be recovered with relative reliability. Inversion with ellipsoid- and elliptic-section pipe models recovered consistent and stable magnetisation direction estimates of inclination −67°, declination 0° in a geomagnetic field of inclination −62°, declination 11°. The departure of the resultant magnetisation from the geomagnetic field (ARRA) of 12° is sufficient to suggest that the magnetisation is not completely induced, but small enough that the centre of magnetisation should be reasonably estimated by modelling with an assumed induced magnetisation only.

Figure 1.12 shows three alternative source models derived by different inversions. Figure 1.12A shows thresholded and isosurface displays of a voxel inversion assuming induced magnetisation performed with the UBC (University of British Columbia) 3D inversion code. As described previously, neither the threshold or isosurface displays faithfully represent the magnetisation that causes the anomaly. Figure 1.12B shows two parametric models: an ellipsoid and a plunging elliptic-section pipe, both of homogeneous magnetisation that is directed

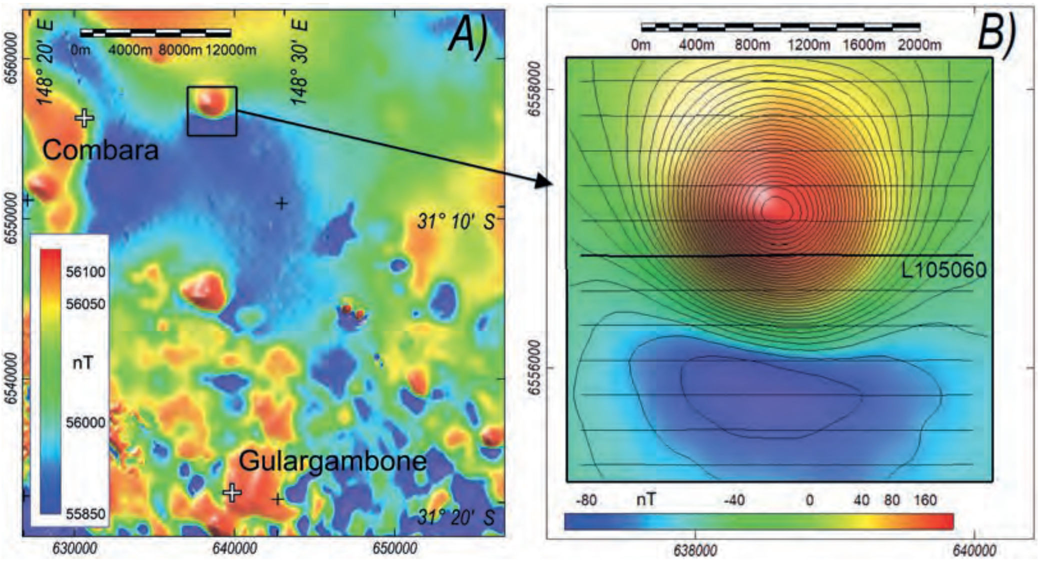

Fig. 1.11. A) part of the TMI map from a regional aeromagnetic survey in New South Wales, Australia and B) detail of a selected anomaly.

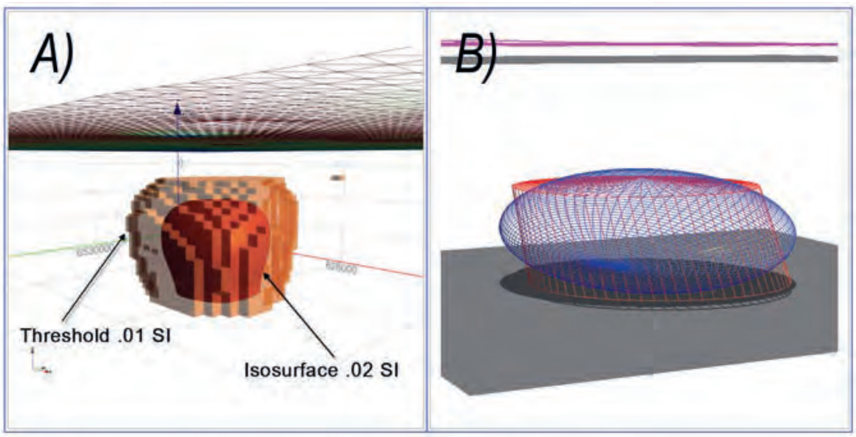

Fig. 1.12. A) 3D Isosurface and threshold representations of a voxel model inversion of the anomaly in Fig. 1.11B, and B) alternative ellipsoid (blue) and elliptic-section pipe (red) models.

slightly away from the local geomagnetic field. However, difference in magnetisation direction plays only a small role in difference between the voxel and parametric models. Figure 1.13 shows the very close fits to the measured field of the computed fields from both parametric models in Fig. 1.12B. No significance can be ascribed to the different post-inversion residual data misfits of the models and it is not feasible to discriminate between the model fields according to their success in matching the measured field. The magnetisation directions and centres of magnetisation of the two parametric models are almost identical. There is a difference of 13% in depth below surface to the top of the two models due to the details of their differences in shape. Only the horizontal-topped pipe model is suitable for depth estimation (the voxel model is also excluded from depth analysis). Shape and depth to the top of a magnetisation are details that are poorly constrained by inversion. The direction of magnetisation and its effective horizontal centre are more reliably determined for this and most compact magnetisations.

Figure 1.14A shows cross-sections on Flightline 105060 through the centre of the anomaly (for location see Fig. 1.11) for the best-fit ellipsoid model (in green) with a magnetisation of 3.8 A/m, and for models with magnetisations double that (in red) and half

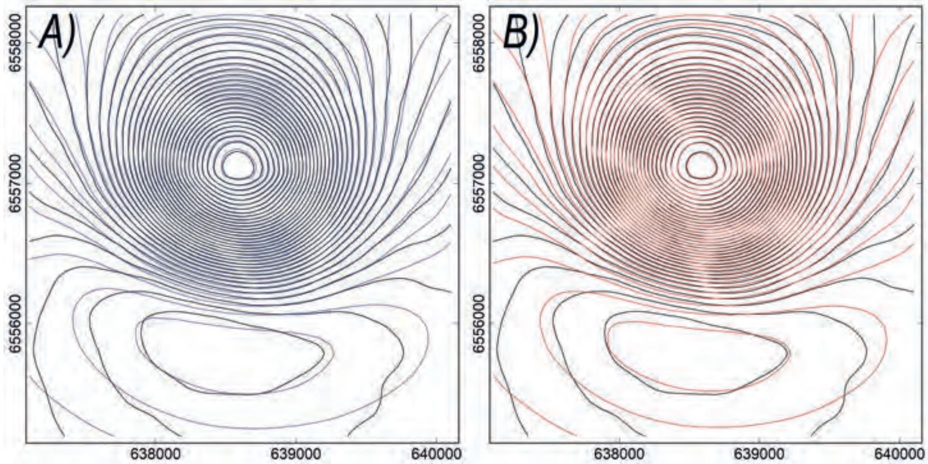

Fig. 1.13. TMI contours: (black) measured and A) (blue) computed from the best ellipsoid inversion model and B) (red) computed from the best elliptic pipe inversion model.

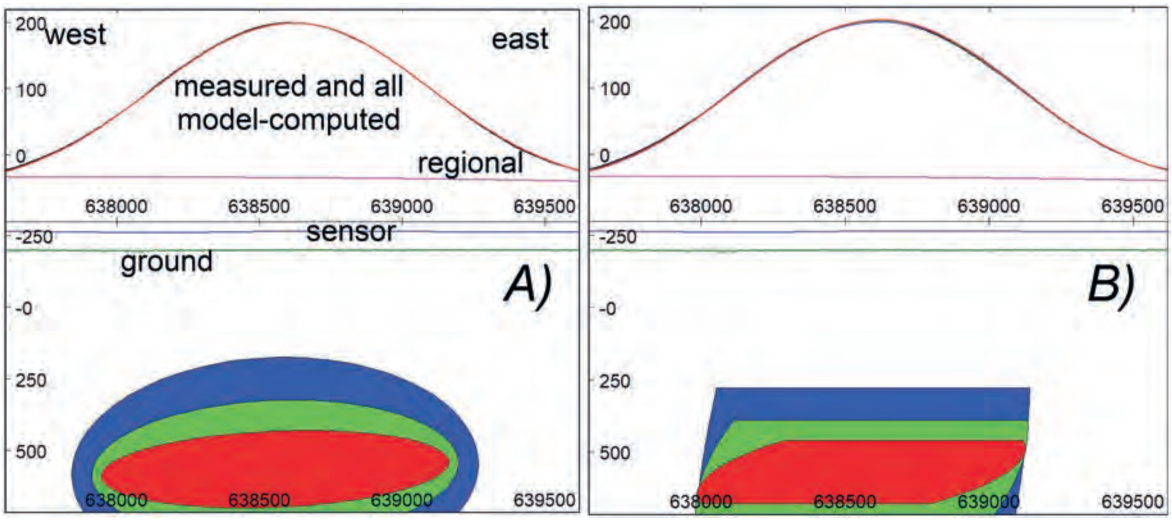

Fig. 1.14. Model sections through flightline 105060 (for location see Fig. 1.11B). A) the best ellipsoid model (red), best-fit ellipsoid of half the susceptibility (blue) and twice the susceptibility (green), and B) the matching set of elliptic pipe models.

of that (in blue). As shown, the computed fields all almost completely match the measured field. Figure 1.14B shows the sections and data-fits for the corresponding pipe models (the best pipe model has a magnetisation of 5.0 A/m. It is not feasible to discriminate between these models based on their goodness of fit to the measured field. Note that this indeterminacy in intensity of magnetisation applies equally to voxel models and discredits any claim that those inversions map detail of variation in magnetisation from voxel to voxel.

Figure 1.15 shows a cross-plot of intensity of magnetisation against volume for a series of ellipsoid and elliptic-section pipe models. The range of the figure spans more than an order of magnitude in both volume and intensity of magnetisation, with very little ground for confidently selecting a value for either parameter. However, the two curves plotted of constant magnetic moment (best estimated as 15.6 A/m^2 for the ellipsoid models and 16.3 A/m^2 for the elliptic-section pipe models show that all bodies have a magnetic moment very close to 16 A/m^2, regardless of their type or individual magnetisation and volume values. This compound parameter of magnetic moment is therefore much more reliably determined from the inversions than the individual parameter values and is a more suitable statistic than intensity of magnetisation or apparent magnetic susceptibility to summarise the source magnetisation for the anomaly.

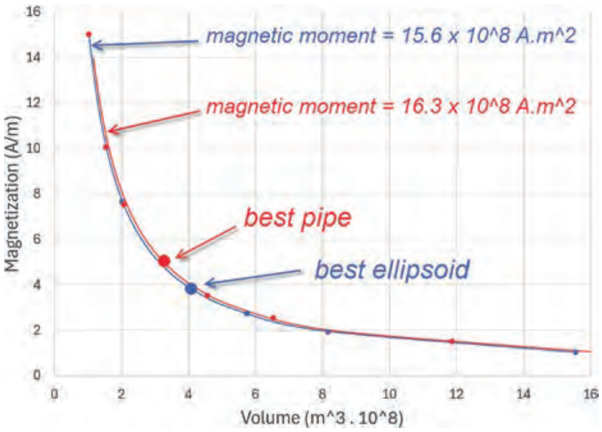

Fig. 1.15. Cross plot of intensity of magnetisation against volume for pipe and ellipsoid models.

1.5.2 The relationship between models and magnetic field anomalies

As has been extensively discussed above, the relationship between models and magnetic fields is extremely anisotropic with an exact relationship in the 'forward' direction and substantial non-uniqueness in the 'reverse' direction. The challenge of the inverse relationship that we mostly deal with is of optimising information recovery of the most reliable model statistics that are made on the basis of justified assumptions and of attributing those recovered statistics with realistic indications of their reliability. The statistics and their reliability estimates are fundamentally constrained by the geology and magnetic field measurements. The apparent detail of parametric and voxel models are very different but if models from well-conducted parametric and voxel inversions are distilled to key statistics, those statistics should be similar.

1.6 MAGNETIC FIELD STUDIES IN MINERAL EXPLORATION

Many mineral deposits have a magnetic field expression, but with exceptions of extreme amplitude anomalies such as those associated with magnetite deposits, few magnetic field features are diagnostic of mineralisation. A review of the magnetic field expression of different styles of mineralisation is given by Clark *et al.* (2003) and by Dentith and Mudge (2014). Dentith *et al.* (1994) and Dentith (2003) report the geophysical expression of various mineral deposits in Western Australia and South Australia respectively. For several forms of mineralisation (e.g. the search for kimberlites in diamond exploration) magnetic field surveys may be a primary exploration method, but in many cases aeromagnetic surveys are used to map the major distribution of geology and structures in an area and provide context to optimise location of exploration methods such as detailed gravity surveys, induced polarisation (IP) and electromagnetics that are more expensive but may also be more diagnostic of mineralisation. Many magnetic field expressions associated with mineralisation are indirect and interpretive, for instance the presence of demagnetised zones caused by alteration, recognition of magnetic field patterns characteristic of deposits, or tracing of the intersection of geological units with structural features. Some magnetic field expressions of mineralisation might be overlooked (e.g. a low amplitude anomaly due to a large body of haematite where the expectation was for a magnetite body) and some forms of mineralisation have no associated magnetisation contrasts and therefore no magnetic field expression. The most common disappointments in application of magnetic field studies to mineral exploration occur in 'bump hunting' where a magnetic field anomaly may be targeted because it is the most prominent anomalous feature in an area. This approach to mineral exploration is most likely to be successful if proven nearby mineralisation is associated with similar magnetic anomalies. The most sophisticated and generally most successful application of magnetic field interpretation in mineral exploration is in construction of geological maps in association with all other available information, supplemented with quantitative modelling or inversion studies where appropriate. In an increasing number of countries around the world, government- or state-funded regional aeromagnetic surveys are flown to provide data sufficient to encourage and enable mineral exploration companies to investigate large areas within which they can selectively commit to exploration tenements where they will perform exploration activities, possibly including more detailed magnetic field surveys to better constrain features of interest.

1.6.1 Aeromagnetic surveys

Most of the magnetic field data used in mineral exploration are measured on aeromagnetic surveys. Application of these data in exploration geophysics started in the late 1940s after wartime development of the technique for submarine detection. Early surveys used vertical component magnetometers but these were soon replaced with total field instruments. Methods of aeromagnetic surveying are described by Gunn (1997) and Reeves (2005) and details of the current technologies can be found from inspection of acquisition reports of recent surveys. Magnetometers have developed considerably over the last 50 years but the most influential advance was the introduction of differential global satellite positioning (DGPS) in the mid-1990s. Before that, positioning was largely by flight recovery from photographs or installing beacons for triangulation. It was only with advent of DGPS that mapping magnetic fields across large areas at high resolution became feasible. Regional surveys that had been flown at 1 km or 1 mile line spacing or greater were reduced to 200 or 400 m line spacing and could subsequently be infilled with detailed surveys at 50 m spacing or closer if required. Many early surveys used magnetometers deployed in a 'bird' towed behind a plane or beneath a helicopter to reduce the magnetic noise associated with the aircraft. However, with much improved magnetic cleaning of aircraft and compensation for their fields, most aeromagnetic data is now acquired with magnetometers in 'stingers' attached to the nose or rear of an aircraft or to the skids of a helicopter. Compensation for aircraft orientation and manoeuvre noise is generally performed using a three-dimensional set of fluxgate vector sensors that are highly sensitive to orientation. This system is calibrated before a survey using a 'comp-box' of data for aircraft roll, pitch and yaw flown at high elevation in the principal survey line directions. Acquisition of this data is highly specialised and is mostly performed by contract companies that maintain specialist aircraft and instruments and employ pilots experienced in flying these surveys, instrument engineers and data processors. On larger surveys client companies employ independent consultants to oversee data acquisition and ensure that all data are of required standard before the contractor leaves the survey area.

Fixed-wing aircraft are most economic for large areas of modest topography. Data are typically acquired at 10 or 20 hertz that equates to spacings of 5 to 10 m according to flight speed. Helicopters are used for smaller surveys or in areas of more rugged terrain. Surveys by either fixed-wing or helicopter are generally specified in terms of constant ground clearance (except where legally mandated over residences or roads) but if there is substantial terrain there are generally advantages in reducing abrupt changes from line to line by flying a 'smooth drape' rather than maintaining constant ground clearance. This includes consistency in flying in the up and down directions over major terrain features that requires considerable skill of the pilot. To reduce abruptness of turn, surveys are not generally flown sequentially along adjacent lines but in a 'racetrack' pattern, with turns between lines performed outside the area of required coverage.

The magnetic field varies in the time that it takes to fly a survey. These time variations are referred to as diurnal variation. On 'quiet' days they follow a common pattern according to the survey latitude, proximity to the ocean and regional variations in crustal and mantle conductivity. However, the variations are not predictable in detail and must be measured at a fixed base station so that they can be subtracted from the same variations experienced by the survey magnetometer. Typical 'quiet day' diurnal variations have ranges of 50 to 100 nT but amplitude and details vary from day to day. There are also days with magnetic storms that occur when flares from sunspot activity and coronal mass ejections impact the Earth. These introduce streams of charged particles that disturb the balance in the Earth's magnetosphere and cause high-amplitude, sharp magnetic field variations that are most severe towards the poles where associated visual effects are known as aurora. It is not feasible to reliably remove these extreme variations from the magnetic field data and surveys must be suspended over these periods. An aeromagnetic survey contract specifies how the level of activity of the field is quantified on the base station records and at what value of a specified variation statistic flying should be suspended. Almost all onshore aeromagnetic surveys are flown in conjunction with acquisition of radiometric data, and following periods of rain when the radiometric signal is supressed there may also be contractual requirements to suspend flying.

REFERENCES

Alken P, Thébault E, Beggan CD, *et al.* (2021) International Geomagnetic Reference Field: the thirteenth generation. *Earth, Planets, and Space* **73**, 49. doi:10.1186/s40623-020-01288-x

Archibald N, Gow P, Boschetti F (1999) Multiscale edge analysis of potential field data. *Exploration Geophysics* **30**, 38–44. doi:10.1071/EG999038

Baranov V (1957) A new method for interpretation of aeromagnetic maps: pseudo-gravimetric anomalies. *Geophysics* **22**, 359–383. doi:10.1190/1.1438369.

Baranov V, Naudy H (1964) Numerical calculation of the formula of reduction to the magnetic pole. *Geophysics* **29**, 67–79. doi:10.1190/1.1439334

Beiki M, Clark DA, Austin JR, Foss CA (2012) Estimating source location using normalized magnetic source strength calculated from magnetic gradient tensor data. *Geophysics* **77**, J23–J37. doi:10.1190/geo2011-0437.1

Biedermann AR, McEnroe SA (2017) Effects of magnetic anisotropy on total magnetic field anomalies. *Journal of Geophysical Research. Solid Earth* **122**, 8628–8644. doi:10.1002/2017JB014647

Blakely RJ (1995) 'Potential theory in gravity and magnetic applications'. Cambridge University Press, pp. 441.

Blakely RJ, Simpson RW (1986) Approximating edges of source bodies from magnetic or gravity anomalies. *Geophysics* **51**, 1494–1498. doi:10.1190/1.1442197

Boschetti F, Hornby P, Horowitz FG (2001) Wavelet based inversion of gravity data. *Exploration Geophysics* **32**, 48–55. doi:10.1071/EG01048

Butler RF (1992) 'Palaeomagnetism: magnetic domains to geologic terrains'. Blackwell Scientific Publications, pp. 238.

Clark DA (2013) New methods for interpretation of magnetic vector and gradient tensor data II: Application to the Mount Leyshon Anomaly, Queensland. *Exploration Geophysics* **44**, 114–127. doi:10.1071/EG12066

Clark DA (2014) Methods for determining remanent and total magnetisations of magnetic sources - a review. *Exploration Geophysics* **45**, 271–304. doi:10.1071/EG14013

Clark DA, Schmidt PW, Coward DA, Huddleston MP (1998) Remote determination of magnetic properties and improved drill targeting of magnetic anomaly sources by Differential Vector Magnetometry (DVM). *Exploration Geophysics* **29**, 312–319. doi:10.1071/EG998312

Clark DA, Genua S, Schmidt PW (2003) Predictive exploration models for porphyry, epithermal and iron-oxide copper-gold deposits: implications for exploration. *AMIRA International Exploration and Mining Report* **1073R**, 398.

Cortés-Ortuño D, Fabian KV, de Groot L (2022) Mapping magnetic signals of individual magnetite grains to their internal magnetic configurations using micromagnetic models. *Journal of Geophysical Research, Solid Earth* **127**, e2022JB024234. doi:10.1029/2022JB024234

Davis A (2022) Nested anisotropic geostatistical gridding of airborne geophysical data. *Geophysics* **87**, E1–E12. doi:10.1190/geo2021-0169.1

Dentith MC (Ed.) (2003) 'Geophysical Signatures of South Australian Mineral Deposits'. ASEG Special Publication 12.

Dentith MC, Mudge ST (2014) 'Geophysics for the mineral exploration geoscientist'. Cambridge University Press, pp. 438.

Dentith MC, Frankcombe KF, Trench A (1994) Geophysical signatures of Western Australian mineral deposits: an overview. *ASEG Extended Abstracts* **1994**(1), 29–54. doi:10.1071/ASEGSpec07_03

Dunlop DJ, Özdemir Ö (1997) 'Rock magnetism: fundamentals and frontiers (Cambridge studies in Magnetism). Cambridge University Press, pp. 596.

Fedi M, Florio G (2001) Detection of potential fields source boundaries by enhanced horizontal derivative method. *Geophysical Prospecting* **49**, 40–58. doi:10.1046/j.1365-2478.2001.00235.x

Foss CA (2017) 'Resultant-magnetization based magnetic field interpretation'. In *Proceedings of Exploration 17: Sixth Decennial International Conference on Mineral Exploration*. (Eds V Tschirhart and MD Thomas) pp. 637–648.

Foss CA, Gouthas G, Fabris A, Werner M, Katona LF, Hutchens M, Reed G (2018) 'Gawler Craton Airborne Geophysical Survey Region 3b, Torrens – Enhanced geophysical imagery and magnetic source depth models'. Report Book 2018/00038. Department for Energy and Mining. South Australia, Adelaide.

Foss CA, Clark DA, Keenan S, Leslie K (2019) Constraining structural dip and magnetization direction of a sheet from its static and dynamic magnetic anomalies. *ASEG Extended Abstracts* **2019**, 1–5. doi:10.1080/22020586.2019.12073127

Foss CA, Gouthas G, Katona LF, Wise TW, Pawley MJ (2019a) 'Gawler Craton Airborne Geophysical Survey Region 4a, Barton – Enhanced geophysical imagery and magnetic source depth models'. Report Book 2019/00012. Department for Energy and Mining. South Australia, Adelaide.

Goldstein NE, Ward SH (1966) The separation of remanent from induced magnetization in situ. *Geophysics* **31**, 779–796. doi:10.1190/1.1439810

Grauch VJS, Cordell L (1987) Limitations of determining density or magnetic boundaries from the horizontal gradient of gravity or pseudogravity data. *Geophysics* **52**, 118–121. doi:10.1190/1.1442236

Gunn PJ (Ed.) (1997) 'Airborne magnetic and radiometric surveys'. *AGSO Journal of Geology and Geophysics* **17**(2).

Hinze W, Von Frese R, Saad A (2013) 'Gravity and Magnetic Exploration: Principles, Practices, and Applications. Cambridge: Cambridge University Press. doi:10.1017/CBO9780511843129

Hornby P, Boschetti F, Horowitz FG (1999) Analysis of potential field data in the wavelet domain. *Geophysical Journal International* **137**, 175–196. doi:10.1046/j.1365-246x.1999.00788.x

Hrouda F (1982) Magnetic anisotropy of rocks and its application in geology and geophysics. *Geophysical Surveys* **5**, 37–82. doi:10.1007/BF01450244

Hrouda F (2007) 'Magnetic susceptibility, anisotropy'. In *Encyclopedia of Geomagnetism and Paleomagnetism*. (Eds D Gubbins, E Herrero-Bervera) pp. 546–560.

Isles DJ, Rankin LR (2013) 'Geological interpretation of aeromagnetic data'. Australian Society of Exploration Geophysicists, pp. 365.

Kasama T, McEnroe SA, Ozaki N, Kogure T, Putis A (2004) Effects of nanoscale exsolution in hematite-ilmenite on the acquisition of stable remanent magnetization. *Earth and Planetary Science Letters* **224**, 461–475. doi:10.1016/j.epsl.2004.05.027

Kellogg OD (1967) 'Foundations of potential theory'. Springer-Verlag, pp. 383.

Koyama T, Kaneko T, Ohminato T, Yanagisawa T, Watanabe A, Takeo M (2013) An aeromagnetic survey of Shinmoe-dak volcano, Kirishima, Japa, after the 2011 eruption using an inmanned autonomous helicopter. *Earth, Planets, and Space* **65**, 657–666. doi:10.5047/eps.2013.03.005

Kuwahata A, Kitaizumi T, Saichi K, *et al.* (2020) Magnetometer with nitrogen-vacancy center in a bulk diamond for detecting magnetic nanoparticles in biomedical applications. *Scientific Reports* **10**, 2483. doi:10.1038/s41598-020-59064-6

Lelièvre PG, Oldenburg DW (2009) A 3D total magnetization inversion applicable when significant, complicated remanence is present. *Geophysics* **74**, L21–L30. doi:10.1190/1.3103249

Li Y, Oldenburg DW (1996) 3D inversion of magnetic data. *Geophysics* **61**, 394–408. doi:10.1190/1.1443968

Li Y, Oldenburg DW (1998) Separation of regional and residual magnetic field data. *Geophysics* **63**, 431–439. doi:10.1190/1.1444343

Löhr SC, Murphy DT, Nothdurft LD, Bolhar R, Piazolo S, Siegel C (2017) Maghemite soil nodules reveal the impact of fire on mineralogical and geochemical differentiation at the earth's surface. *Geochimica et Cosmochimica Acta* **200**, 25–41. doi:10.1016/j.gca.2016.12.011

Lourenço JS, Morrison HF (1973) Vector magnetic anomalies derived from measurements of a single component of the field. *Geophysics* **38**, 359–368. doi:10.1190/1.1440346

MacMillan WD (1930) 'The theory of the potential'. Dover Publications, New York, pp. 324.

Nabighian MN (1972) The analytic signal of two-dimensional magnetic bodies with polygonal cross-section: its properties and use for automated anomaly interpretation. *Geophysics* **37**, 505–517. doi:10.1190/1.1440276

Naprstek T, Smith RS (2019) A new method for interpolating linear features in aeromagnetic data. *Geophysics* **84**, JM15–JM24. doi:10.1190/geo2018-0156.1

Pastore Z, Church NS, McEnroe SA (2019) Multistep parametric inversion of scanning magnetic microscopy data for modelling magnetization of multidomain magnetite. *Geochemistry, Geophysics, Geosystems* **20**, 5334–5351. doi:10.1029/2019GC008542

Purss MBJ, Cull JP (2005) A new iterative method for computing the magnetic field at high magnetic susceptibilities. *Geophysics* **70**, L53–L62. doi:10.1190/1.2052469

Reeves C (2005) 'Aeromagnetic surveys: Principles, practice and interpretation'. Earth-works, Washington DC, 155 p.

Reid AB (1980) Aeromagnetic survey design. *Geophysics* **45**, 895–982. doi:10.1190/1.1441102

Robinson P, Harrison RJ, McEnroe SA, Hargraves RB (2002) Lamellar magnetism in the hematite-ilmenite series as an explanation for strong remanent magnetization. *Nature* **418**, 517–520. doi:10.1038/nature00942

Roest WR, Verhoef J, Pilkington M (1992) Magnetic interpretation using the 3-D analytic signal. *Geophysics* **57**, 116–125. doi:10.1190/1.1443174

Schiffler M, Queitsch M, Stoltz R, Chwala A, Krech W, Meyer HG, Kukowski N (2014) Calibration of SQUID vector magnetometers in full tensor gradiometry systems. *Geophysical Journal International* **198**, 954–964. doi:10.1093/gji/ggu173

Schmidt PW (2015) The Qmeter - a portable tool for remanence and susceptibility. *ASEG Extended Abstracts* **2015**(1), 1–3. doi:10.1071/ASEG2015ab235

Schmidt PW, Lackie MA (2014) Practical considerations: making measurements of susceptibility, remanenec and Q in the field. *Exploration Geophysics* **45**, 305–313. doi:10.1071/EG14019

Schmidt PW, Clark DA, Leslie KE, Bick M, Tilbrook D, Foley C (2004) GETMAG – a SQUID magnetic tensor gradiometer for mineral and oil exploration. *Exploration Geophysics* **35**, 297–305. doi:10.1071/EG04297

Schmidt PW, McEnroe SA, Clark DA, Robinson D (2007) Magnetic properties and potential field modelling of the Peculiar Knob metamorphosed iron formation, South Australia: an analogue for the source of the intense Martian magnetic anomalies? *Journal of Geophysical Research* **112**, B03102. doi:10.1029/2006JB004495

Wijns C, Perez C, Kowlczyk P (2005) Thetamap: edge detection in magnetic data. *Geophysics* **70**, L39–L43. doi:10.1190/1.1988184

This page intentionally left blank